Received: 24 March 2025 | Revised: 13 July 2025 | Accepted: 17 September 2025

DOI: 10.1111/jori.70024

ORIGINAL ARTICLE

Journal of Risk and Insurance

Optimal hedging of longevity risks for group self-annuity portfolios

Yang Shen | **Michael Sherris** | **Yawei Wang** | **Jonathan Ziveyi**

School of Risk and Actuarial Studies, ARC Centre of Excellence in Population Ageing Research (CEPAR), UNSW Sydney, Sydney, New South Wales, Australia

Correspondence
Yawei Wang, School of Risk and Actuarial Studies, ARC Centre of Excellence in Population Ageing Research (CEPAR), UNSW Sydney, NSW 2052, Australia.
Email: yawei.wang@unsw.edu.au

Abstract

This paper proposes a dynamic longevity risk hedging strategy for smooth survival benefit profiles of group self-annuity (GSA) schemes in the presence of population basis risk. The fund manager of GSA acts on behalf of fund participants in selecting the optimal hedge. The hedging framework is formulated as a mean-variance optimization problem, which serves as a theoretical framework for selecting the optimal hedging strategy. The hedging mechanism involves trading standardized longevity-linked securities dynamically. A semi-analytic solution to the optimal hedge ratio is derived, which enhances the numerical implementation of the strategy. Furthermore, a risk decomposition method is developed, enabling hedging of various sources of risks, such as longevity and investment risks. Numerical illustrations highlight that the hedging strategy effectively mitigates variability in survival benefits. Meanwhile, a holistic risk management framework utilizing the longevity risk hedging strategy and a target volatility investment strategy increases the fund's return per unit of risk.

KEYWORDS

group self-annuity, hedging, investment risk, longevity risk, population basis risk, retirement income products, risk-pooling

JEL CLASSIFICATION
G11, G22, J32

1 | INTRODUCTION

Life expectancy has been increasing globally, albeit with occasional adverse longevity shocks such as the COVID-19 pandemic (World Health Organization, 2024). This upward trend places increasing pressure on public pension systems, especially with the widespread shift from defined benefit to defined contribution schemes (Mantilla-Garcia et al., 2024). Consequently, retirees have to manage all risks, including longevity, investment, and inflation (Konicz & Mulvey, 2015; Owadally et al., 2021). This paper focuses primarily on longevity risk while considering investment risk management as an extension of the hedging framework.

Theoretically, purchasing an annuity is the optimal solution for transferring individual longevity risk to an annuity provider (Yaari, 1965). However, the annuity market remains underdeveloped (Brown, 2007), largely due to issues such as adverse selection and capital requirements, which drive up premiums (Evans & Sherris, 2010; Friedman & Warshawsky, 1990). Additionally, annuities tend to be illiquid and inflexible, further deterring retirees' demand for them (Hurd, 1989; Pitacco, 2016).

A promising alternative is the pooling of longevity risk. Risk-pooling products allow members to convert a lump sum into lifetime income while redistributing the remaining balance of deceased participants among survivors. Several such products have been proposed, for example, group self-annuities (GSAs) (Piggott et al., 2005; Qiao & Sherris, 2013), pooled annuity funds (Donnelly et al., 2014; Stamos, 2008), and tontines (Chen et al., 2021; Milevsky, 2014; Milevsky & Salisbury, 2015; Weinert & Gründl, 2021). These arrangements eliminate the need for insurance premiums and capital reserves, reducing adverse selection and improving postretirement utility (Chen et al., 2021; Hanewald et al., 2013; Shen et al., 2023; Valdez et al., 2006). Notable examples include the QSuper Lifetime Pension[1] in Australia and the GuardPath Modern Tontine[2] in Canada.

Despite their advantages, risk-pooling products face two key challenges due to systematic longevity risk. First, as life expectancy increases, survival payments decrease. Second, these benefits are volatile due to uncertainty in future mortality rates.[3] Strategies such as dynamic pooling (Qiao & Sherris, 2013) and target volatility investment strategy (Bégin & Sanders, 2024; Li et al., 2022; Olivieri et al., 2022) can increase the effectiveness of the GSA schemes. This paper extends the existing literature by proposing a novel dynamic hedging framework that leverages standardized longevity securities to stabilize GSA survival benefits. Our approach can be generalized to other pooling schemes (see Remark 3.4) and integrates investment risk management through a risk decomposition method. Fund managers can implement this hedging framework and target volatility investment strategies[4] concurrently to make benefit profiles more appealing.

[1] https://qsuper.qld.gov.au/our-products/superannuation/lifetime-pension.

[2] https://www.guardiancapital.com/investmentsolutions/guardpath-modern-tontine-trust/.

[3] Additional sources of volatility include unsystematic longevity risk, which arises from small pool sizes, and investment risk, which stems from fluctuations in the return of the underlying fund (Piggott et al., 2005). We assess the impact of pool size on hedging effectiveness in Section 4.3.4.

[4] Section 5 presents several target volatility investment strategies and their integration into a holistic risk management framework.

The growing longevity risk transfer market underscores the importance of index-based longevity securities (Blake et al., 2019). Since J.P. Morgan and Lucida executed the first q-forward transaction in 2008, market participants have increasingly recognized the value of instruments such as longevity bonds (Blake & Burrows, 2001), longevity swaps (Dowd et al., 2006), q-forwards (Coughlan et al., 2007), S-forwards (Coughlan et al., 2013), K-forwards (Tan et al., 2014), e-forwards (Denuit, 2009), mortality options (Cairns et al., 2008), survival options (Dowd, 2003), among others. While extensive research has explored their use in hedging annuity portfolios and defined benefit pension plans (Cairns, 2011, 2013; Li & Hardy, 2011; Li & Luo, 2012; Tan et al., 2022; Wong et al., 2017; Zhou & Li, 2017, 2019), their application to longevity pooling products remains largely unexplored.

Index-based longevity securities offer cost-effective hedging solutions and enable dynamic risk management. However, they are limited by the population basis risk, which is the mismatch between the hedged population and the reference population of the securities (Blake, 2018; Cairns et al., 2014; Coughlan et al., 2011; Li & Hardy, 2011; Lin et al., 2014; Rosa et al., 2017; Tan et al., 2022; Zhou & Li, 2017, 2019). Among the available instruments, longevity swaps are the most widely traded (Blake et al., 2019), with a cumulative transaction volume of US $250 billion as of December 2023[5] (see Figure 1). In this paper, we use the S-forward, which is the basic building block for a longevity swap, to hedge against an unexpected change in mortality to preserve a more stable income for the GSA members in the presence of population basis risk.

The hedging framework for longevity risk can be categorized into three types: static, continuous-time dynamic, and discrete-time dynamic hedging. Static hedging involves setting up a portfolio at the beginning and holding it unchanged (Cairns, 2013; Li & Hardy, 2011; Ngai & Sherris, 2011; Sherris et al., 2020). Static hedging is easy to implement but lacks adaptability and requires index-based longevity securities with a long time-to-maturity to match the duration of the hedged position. Continuous-time dynamic hedging allows continuous rebalancing (Biagini et al., 2016, 2013; Dahl et al., 2008; Dahl & Møller, 2006; Wong et al., 2014, 2017), yet it is impractical due to the need for frequent trades. The third approach, discrete-time dynamic hedging (Cairns, 2011, 2013; Luciano et al., 2012; Rosa et al., 2017; Tan et al., 2022; Zhou & Li, 2017, 2019), periodically adjusts the portfolio (e.g., annually). This method balances flexibility and feasibility, and is typically based on mortality models from the Lee-Carter (Lee & Carter, 1992) or Cairns–Blake–Dowd (Cairns et al., 2006) families. Given practical considerations, we adopt a discrete-time dynamic hedging approach for GSAs.

To account for population basis risk, we adopt a multi-population mortality model[6] proposed in Li and Lee (2005). We show that, due to the payout structure of GSAs and the risk premium charged on the S-forwards, hedging introduces a mean-variance trade-off for fund members: while variance reduction stabilizes benefits, it also lowers expected payouts. Therefore, the hedging objective is to optimize this trade-off. To achieve this, we construct a one-step-ahead hedging strategy (Alizadeh et al., 2008) that aligns with the economic interests of GSA members. We derive semi-closed-form solutions for the mean-variance set and the optimal hedge ratio, allowing fund managers to select an efficient portfolio of S-forwards and

[5]Data source: https://www.artemis.bm/longevity-swaps-and-longevity-risk-transfers/.

[6]Some other multi-population models include the multi-population Lee-Carter (M-LC) model (Cairns et al., 2011), the multi-population Cairns–Blake–Dowd (M-CBD) model (Li et al., 2015), and the common age effect model (Kleinow, 2015), among others.

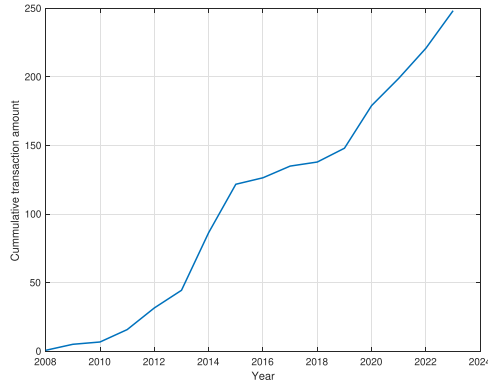

FIGURE 1 The cumulative amount of longevity swap transactions in US$ billion since 2008. Data source: https://www.artemis.bm/longevity-swaps-and-longevity-risk-transfers/. [Color figure can be viewed at wileyonlinelibrary.com]

the GSA fund from the efficient set. The efficient set is conceptually similar to the capital market line in portfolio selection theory (Markowitz, 1952), where investors choose between risk-free assets and a market portfolio. We measure the effectiveness of the hedge through the variance reduction ratio (VRR) (Li & Hardy, 2011; Tan et al., 2022; Zhou & Li, 2017), which quantifies how the hedge can remove the variance of survival payments. The cost of the hedge is captured by the mean reduction ratio (MRR), which measures the extent to which the hedge decreases the expected survival benefit.

Numerical analysis reveals that: (i) fund members select the hedging strategy from the efficient set, which is the upper curve of the parabola; (ii) more risk-averse members prefer strategies closer to the global minimum variance point (GMVP); (iii) a significant proportion of longevity risk can be eliminated by implementing our dynamic hedging framework; (iv) the hedge provides a net gain to members, with benefits exceeding the associated cost. Sensitivity analysis confirms that the effectiveness of the dynamic hedge is robust to the S-forwards' reference age and time-to-maturity, the hedger's population, interest rate risk, the pool size of the GSA, and model risk. Additionally, we propose a risk decomposition method to jointly manage longevity and investment risks, improving return per unit of risk relative to standalone investment risk management strategies.

This paper makes three key contributions. First, while longevity hedging strategies have been extensively studied for annuity portfolios, this paper is the first to apply standardized index-based longevity securities to risk-pooling products. The semi-analytic solutions facilitate practical implementation. Second, we introduce a novel risk decomposition method that enables fund managers to quantify and manage different sources of risks, including longevity and investment risks. Third, we show that several target volatility strategies proposed in literature (Doan et al., 2018; Li et al., 2022; Olivieri et al., 2022) are mathematically equivalent.

The remainder of this paper is structured as follows: Section 2 presents the model setup, including the mortality model, the GSA, and the S-forward. Section 3 formulates the dynamic hedging problem and provides semi-analytic solutions. Section 4 provides numerical results and robustness checks. Section 5 extends the framework to incorporate investment risk. Concluding remarks are presented in Section 6. Appendices contain proofs, computational methods, and parameter estimates.

2 | MODEL SETUP

We fix the probability space $(\Omega, \mathcal{F}, \mathbb{P})$ equipped with a right-continuous, $\mathbb{P}$-completed filtration $\mathbb{F} := \mathcal{F}_{t\in[0,T]}$, where T is the maximum remaining life span of a person aged x at time zero. Let $\{\epsilon_{x,t}^{(F)}, \epsilon_{x,t}^{(R)}, \xi_t, \zeta_t^{(F)}, \zeta_t^{(R)}\}_{t\in[0,T]}$ be a sequence of mutually independent and identically distributed (IID) normal random variables with zero mean and constant variances on $(\Omega, \mathcal{F}, \mathbb{F}, \mathbb{P})$, which will be used to describe the mortality dynamics in Section 2.1. Let $\{W_t^1, W_t^2\}_{t\in[0,T]}$ be a pair of independent standard Brownian motions on $(\Omega, \mathcal{F}, \mathbb{F}, \mathbb{P})$, which will be used to describe stock dynamics in Section 5. In this paper, we assume that the financial market and human mortality are independent (Feng et al., 2025), that is, $\{\epsilon_{x,t}^{(F)}, \epsilon_{x,t}^{(R)}, \xi_t, \zeta_t^{(F)}, \zeta_t^{(R)}\}_{t\in[0,T]}$ and $\{W_t^1, W_t^2\}_{t\in[0,T]}$ are mutually independent. In Sections 2–4, we focus on the systematic longevity risk and assume that the fund of the risk-pooling products is fully invested in a risk-free bank account. We relax this assumption and allow for investment risk in Section 5.

2.1 | The mortality model

The hedging framework requires a stochastic mortality model to derive the optimal hedge ratio. Cairns (2011) adopts a single population setup and uses the Cairns–Blake–Dowd mortality model (Cairns et al., 2006) in hedging a portfolio of annuity liabilities. In this paper, we use the augmented common factor (ACF) model proposed in Li and Lee (2005) and assume two populations. The reference population, R, is the total population, and the hedging population is denoted as F. The hedging population is the book population of the risk-pooling products. It can be a sub-population of Population R or another population resembling similar mortality trends. The book population (Population F) aims to hedge the systematic longevity risk.

Let $m_{x,t}^{(i)}$ be the central death rate for Population i at time t, where $i \in \{F, R\}$. In the ACF model, Population i's mortality rate $m_{x,t}^{(i)}$ is determined as:

$$\log\left(m_{x,t}^{(i)}\right) = a_x^{(i)} + G_x K_t + g_x^{(i)} k_t^{(i)} + \epsilon_{x,t}^{(i)}, \tag{1}$$

where $a_x^{(i)}$ is the average mortality rate for an individual aged x from Population i, K_t and $k_t^{(i)}$ are time-varying indices describing the mortality trend for both populations and Population i respectively, G_x and $g_x^{(i)}$ are shape parameters to reflect the sensitivity to the time-varying indices for age x, and $\epsilon_{x,t}^{(i)}$ is the error term modeled by IID normal random variables. The time-varying indices and shape parameters are subject to the following constraints to guarantee the identifiability of the ACF model:

$$\sum_x G_x = \sum_x g_x^{(i)} = 1,$$
$$\sum_t K_t = \sum_t k_t^{(i)} = 0.$$

In the ACF model, $G_x K_t$ is the common factor for the two populations, and $g_x^{(i)} k_t^{(i)}$ is the specific factor for Population i. The mortality rates between the two populations are correlated through the common factor. However, the correlation is not perfect, as there is a specific factor

for each population. We use an index I_t to measure the population basis risk (Zhou & Li, 2017), which is defined as:

$$I_t := \frac{\mathrm{Var}_t\left(g_{x+t}^{(F)} k_{t+1}^{(F)}\right)}{\mathrm{Var}_t(G_{x+t} K_{t+1})}.$$

The index I_t measures the imperfect correlation and quantifies the relative importance of the population-specific factor of the book population in the ACF model.

Following Li and Lee (2005), we assume that the time-varying index K_t for both populations follows a random walk with drift and the time-varying index $k_t^{(i)}$ for Population i follows a first-order autoregressive process:

$$K_t = C + K_{t-1} + \xi_t, \tag{2}$$

$$k_t^{(i)} = \phi_0^{(i)} + \phi_1^{(i)} k_{t-1}^{(i)} + \zeta_t^{(i)}, \tag{3}$$

where $C, \phi_0^{(i)}$, and $\phi_1^{(i)}$ are constants, $\{\xi_t\}$ is a sequence of IID normally distributed random variables with zero mean and constant variance σ_K^2, and $\{\zeta_t^{(i)}\}$ is a sequence of IID normal random variables with zero mean and constant variance $\sigma_{k,i}^2$. We require $|\phi_1^{(i)}| < 1$, so that the time-varying indices $\{k_t^{(i)}\}$ are stationary and the projected mortality for the two populations does not diverge to infinity over time. From Equations (2)–(3), the time-varying indices $\{K_t\}$ and $\{k_t^{(i)}\}$ are Markov processes, whose expected future values depend only on their current values but not on past observations.

2.2 | Group self-annuity

In this subsection, we introduce the fund process of a group self-annuity (GSA) and explain why the participants in the GSA pool are willing to hedge systematic longevity risk. The fund members are from the book Population F.

First, we introduce some notation for survival probabilities. Let $q_{x,t}^{(i)}$ be the probability that an individual aged x in Population i at time $t-1$ dies during the period $[t-1, t)$, which is determined as:

$$q_{x,t}^{(i)} = 1 - \exp\left(-m_{x,t}^{(i)}\right),$$

where $m_{x,t}^{(i)}$ is the central death rate in the ACF model in Equation (1). Let $S_{x,t}^{(i)}(s)$ be the survival probability that an individual aged x in Population i at time t survives to time $t+s$ and this is denoted as:

$$S_{x,t}^{(i)}(s) = \prod_{j=1}^{s} \left(1 - q_{x+j-1,t+j}^{(i)}\right).$$

Here, the survival probability $S^{(i)}_{x,t}(s)$ is random and is not observable until time $t + s$. The randomness comes from the error terms $\{\xi_t, \zeta^{(F)}_t, \zeta^{(R)}_t\}$ in the ACF model. Due to the Markov property of the processes $\{K_t\}$, $\{k^{(F)}_t\}$ and $\{k^{(R)}_t\}$, we have

$$p^{(i)}_{x,t}\left(s, K_t, k^{(i)}_t\right) := \mathbb{E}\left[S^{(i)}_{x,t}(s) \middle| \mathcal{F}_t\right] = \mathbb{E}\left[S^{(i)}_{x,t}(s) \middle| K_t, k^{(i)}_t\right], \tag{4}$$

where $p^{(i)}_{x,t}$ is the spot survival probability that an individual aged x in Population i at time t survives to time $t + s$.

We consider a homogeneous GSA pool consisting of n members initially aged x with each member contributing a lump sum of c to the fund, and assume that the GSA fund invests in risk-free bank accounts. The GSA fund evolves as follows (Piggott et al., 2005; Qiao & Sherris, 2013):

$$N_t = N_{t-1} S^{(F)}_{x+t-1,t-1}(1), \tag{5}$$

$$\Delta N_t = N_{t-1} - N_t,$$

$$F^-_t = F^+_{t-1}(1 + r^f),$$

$$B_t = \frac{F^-_t}{\ddot{a}^e_{x+t,t} N_t}, \tag{6}$$

$$D_t = \beta \frac{F^-_t}{N_{t-1}}, \tag{7}$$

$$F^+_t = F^-_t - B_t N_t - D_t \Delta N_t.$$

The notations in the above GSA fund dynamics are defined as follows:

- N_t is the number of surviving members at time t with $N_0 = n$, and ΔN_t is the number of deaths during $[t - 1, t)$;
- F^-_t is the fund value at time t just before the benefit payment with $F^-_0 = nc$, and F^+_t is the fund value at time t just after the benefit payments;
- r^f is the fixed risk-free interest rate;
- B_t is the GSA survival benefit per member at time t, and $\ddot{a}^e_{x+t,t}$ is the annuity factor taking account of future mortality improvement;
- D_t is the GSA death benefit per member who dies during $[t - 1, t)$, and β is the death benefit payment ratio.

In Equation (6), the annuity factor is determined as:

$$\ddot{a}^e_{x+t,t} = \sum_{s=0}^{+\infty} (1 + r^f)^{-s} p^{(F)}_{x+t,t}\left(s, K_t, k^{(F)}_t\right). \tag{8}$$

We assume that $m_{x,t} = m_{99,t}$ for $x \geq 100$ in the calculation of the annuity factor. At each payment date, the annuity factor is updated based on the latest information $\left\{K_t, k_t^{(F)}\right\}$ in the ACF model. By including future mortality improvements, the expected declining trend of the GSA survival payment could be reduced (Qiao & Sherris, 2013). For the GSA design, we also incorporate death payment in Equation (7) to meet individuals' bequest motives. As noted in Olivieri et al. (2022), we require $0 \leq \beta < 1$ so that the individual longevity risk is shared within the GSA fund. If $\beta = 1$, a member's share of fund value will be fully distributed upon the member's death, and the participants bear all longevity risks themselves. As a result, the GSA fund becomes a pure financial arrangement.

Increasing the pool size can reduce idiosyncratic longevity risk and smoothen the survival benefits of GSA. However, increasing the pool size cannot manage the systematic longevity risk for the group (Qiao & Sherris, 2013). This is because when there is an unexpected systematic improvement in mortality, the life expectancy of all members is expected to increase. In Equation (5), we consider a large pool size so that there is no small sample risk, and the idiosyncratic longevity risk is fully diversified since the research focus is hedging the systematic longevity risk. To test the robustness of the hedging strategy, we perform a sensitivity analysis of hedge effectiveness on the size of the GSA pool in Section 4.3-4.

The systematic longevity risk causes the survival benefits of a GSA pool to be volatile. If the 1-year survival probability $S^{(F)}_{x+t-1,t-1}(1)$ or the annuity factor $\ddot{a}^{e}_{x+t,t}$ increases unexpectedly, the GSA benefit payment B_t will decrease. For this reason, fund members are interested in hedging against unexpected mortality improvements in the future. In addition, the survival benefit B_t is random due to the randomness of the annuity factor $\ddot{a}^{e}_{x+t,t}$ and the 1-year survival probability $S^{(F)}_{x+t-1,t-1}(1)$. Hedging against an unexpected change in mortality can reduce benefit volatility.

2.3 | *S*-forward

In this subsection, we introduce one type of mortality-linked instrument: *S*-forward. We show how to use *S*-forwards to hedge longevity risk in the next section.

An *S*-forward is a combination of a swap and a zero-coupon bond. It is issued on a reference population, and its value is linked to the survival rate of the reference population during a predetermined period. For the swap component, as reflected in Figure 2, two parties will exchange the fixed survival probability and the realized survival probability at maturity. The fixed-rate payer pays the notional amount times the predetermined fixed survival probability to the floating-rate payer. The floating-rate payer pays the notional amount times the realized survival probability to the floating-rate payer. The fixed survival probability is agreed by the two parties at the inception of the *S*-forward. There is no initial cashflow for the two parties when initiating the *S*-forward contract. The *S*-forward is also a zero-coupon bond as it only generates one cashflow at maturity.

Consider an *S*-forward linked to the Population *R* aged x_f. For the *S*-forward issued at time t with a time-to-maturity T^*, its value depends on the reference survival probability $S^{(R)}_{x^f,t}(T^*)$. In practice, the floating-rate payer typically requires a risk premium to accept longevity risk. Let $\lambda \geq 0$ be the risk loading parameter and p_t^f be the forward survival probability at inception, we have

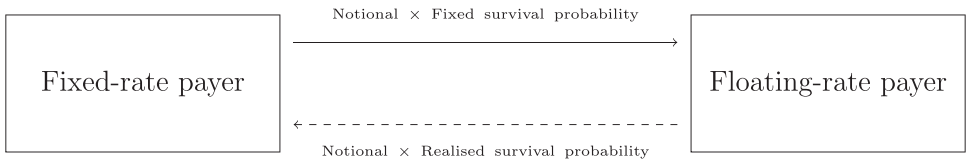

FIGURE 2 Settlement of an S-forward contract at maturity. The fixed-rate payer will make payments to the floating-rate payer based on an initially agreed fixed survival probability, to receive back payments based on the realized survival probability.

$$p_t^f := (1+\lambda)\mathbb{E}\left[S^{(R)}_{x^f,t}(T^*)\middle| K_t, k_t^{(R)}\right].$$

From the fixed-rate payer's perspective, let $P_s(t)$ be the value of the S-forward per \$1 notional at time s, where $s \geq t$. Then $P_s(t)$ can be expressed as:

$$P_s(t) := (1+r^f)^{-(T^*+t-s)}\left\{\mathbb{E}\left[S^{(R)}_{x^f,t}(T^*)\middle| K_s, k_s^{(R)}\right] - p_t^f\right\}. \tag{9}$$

From Equation (9), we have $P_t(t) \leq 0$[7] and $P_s(t)$ is random after inception and before the maturity date $t+T^*$. After inception, the value of the S-forward may become positive or negative depending on the realized mortality over time. If there is an unexpected mortality improvement, the expected survival probability increases, the value of the S-forward increases, and the fixed-rate payer earns a profit. In contrast, if there is an unexpected increase in mortality, the expected survival probability decreases, the value of the S-forward decreases, and the fixed-rate payer incurs a loss. One important result is that the expected return of a fairly priced (i.e., $\lambda = 0$) S-forward is zero for the two parties. This result is natural since there is no cost to enter into the S-forward. In contrast, if a risk premium is charged, the expected return of an S-forward is negative from the fixed-rate payer's perspective, as shown in Proposition 2.1.

Proposition 2.1. *For a fairly priced S-forward, that is, when* $\lambda = 0$, *we have* $\mathbb{E}_t[P_s(t)] = 0$, for $s \geq t$, *where* $\mathbb{E}_t[\cdot] := \mathbb{E}[\cdot|\mathcal{F}_t]$. *If a risk premium is charged by the floating-rate payer* (*i.e.*, $\lambda > 0$), *then* $\mathbb{E}_t[P_s(t)] < 0$, for $s \geq t$.

Proof. See Appendix A.1. □

In the following, we will adopt the same notation for conditional expectation as in Proposition 2.1 for convenience. For example, given the filtration at time t, $\mathrm{Var}_t[\cdot] := \mathrm{Var}[\cdot|\mathcal{F}_t]$ is the conditional variance, $\mathrm{Std}_t[\cdot] := \mathrm{Std}[\cdot|\mathcal{F}_t]$ is the conditional standard deviation, $\mathrm{Cov}_t[\cdot,\cdot] := \mathrm{Cov}[\cdot,\cdot|\mathcal{F}_t]$ is the conditional covariance, and $\mathrm{Corr}_t[\cdot,\cdot] := \mathrm{Corr}[\cdot,\cdot|\mathcal{F}_t]$ is the conditional correlation coefficient.

[7]Although the initial value $P_t(t)$ from the fixed-rate payer's perspective is non-positive, no cashflow is exchanged at inception of the S-forward. A single cashflow occurs at maturity or when the position is closed through offset trading before maturity, as explained in Remark 3.3.

3 | THE OPTIMAL HEDGING FRAMEWORK USING *S*-FORWARD

As detailed in Section 2.2, GSA members are willing to hedge against an unexpected mortality change to smoothen the GSA survival payments. By construction, the GSA survival payments are a series of cashflows, but the S-forwards only generate one cashflow at maturity. Due to the different nature of the cashflows, using only one S-forward to hedge the systematic longevity risk for the GSA members is inadequate. Therefore, it is natural to consider a dynamic hedging strategy that periodically rebalances the hedging portfolio to match the cashflow on each survival payment date. This type of dynamic hedging strategy is commonly used in literature; see, for example, Zhou and Li (2017) and Tan et al. (2022).

In this paper, we assume that the GSA benefits are paid annually.[8] We consider a yearly rolling hedging strategy accordingly, which keeps structuring S-forwards at the beginning of each year and closing out the S-forwards at the end of each year. All the S-forwards used in this hedging strategy are linked to the Population R and age x_f, and their time-to-maturities are T^*. The GSA fund is the fixed-rate payer of the S-forwards. One key feature of the dynamic hedging strategy is that the fund periodically rebalances the hedging portfolio according to the most up-to-date information. More specifically, the yearly rolling hedging strategy works as follows:

- At time $t = 0$, the fund enters into an S-forward contract as the fixed-rate payer with a notional amount h_0 according to the most up-to-date mortality information $\mathcal{F}_0$. The S-forward is issued on the reference population aged x^f at time zero with time-to-maturity T^*.
- At time $t = 1$, the fund closes out the previous S-forward contract. The realized hedging profit or loss is $h_0 P_1(0)$.
- At time $t = 1$, the fund enters into a new S-forward contract as the fixed-rate payer with a notional amount h_1 according to the most up-to-date mortality information $\mathcal{F}_1$. The new S-forward is issued at time $t = 1$ on the reference population aged x^f with time-to-maturity T^*.
- The fund continues to rebalance the hedging portfolio in the same way until maturity.

Figure 3 presents a step-by-step illustration of the yearly rolling hedging strategy.

By implementing the dynamic hedging strategy, the total survival benefit per member $B_{t+1}^{(H)}$ is determined as:

$$B_{t+1}^{(H)} = B_{t+1} + \frac{h_t P_{t+1}(t)}{N_{t+1}} = B_{t+1} + \frac{h_t P_{t+1}(t)}{N_t S_{x+t,t}^{(F)}(1)}, \tag{10}$$

where the realized profit or loss from the S-forward, $h_t P_{t+1}(t)$, is equally distributed among all surviving members. From Equation (9), the hedging profit or loss of the fixed-rate payer per \$1 notional at time $t + 1$ is expressed as:

[8]Existing risk-pooling arrangements include the QSuper Lifetime Pension in Australia and the GuardPath Modern Tontine in Canada have an annual benefit payment frequency.

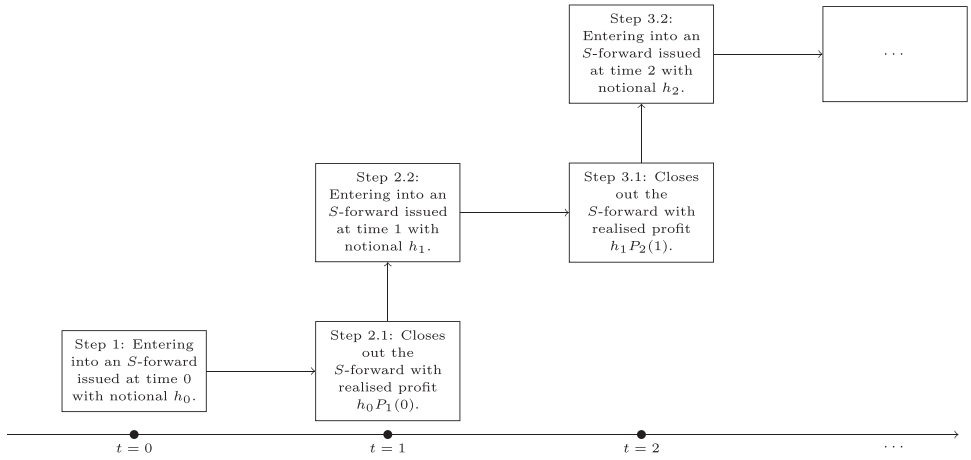

FIGURE 3 The yearly rolling hedging strategy. The GSA fund is the fixed-rate payer of the S-forwards and it keeps rebalancing the hedging portfolio annually. GSA, group self-annuities.

$$\begin{aligned} P_{t+1}(t) &= (1 + r^f)^{-(T^*-1)} \left\{ \mathbb{E}_{t+1}\left[S^{(R)}_{x^f,t}(T^*) \right] - p^f_t \right\} \\ &= (1 + r^f)^{-(T^*-1)} \left\{ S^{(R)}_{x^f,t}(1) \times \mathbb{E}_{t+1}\left[S^{(R)}_{x^f+1,t+1}(T^* - 1) \right] - p^f_t \right\}. \end{aligned} \tag{11}$$

Remark 3.1. We assume that an S-forward indexed to the fund population does not exist in the market, since the fund population F is usually a sub-population. A mortality-linked instrument indexed to a small population is less attractive in the capital market. To increase the liquidity of the mortality-linked instruments, S-forwards are generally indexed to a whole population. This paper assumes that the S-forwards are indexed to the total population R. In the ACF model, the mortality experience between the two populations is correlated, but the correlation is not perfect. Thus, there is a population basis risk for the longevity hedge.

Remark 3.2. To hedge longevity risk, the GSA fund should be the fixed-rate payer of the S-forwards, that is, h_t needs to be positive. When there is an unexpected mortality improvement, from Equation (6), we know that the survival payment will decrease due to the increase in the annuity factor and the number of survival members. Since the mortality experience between the two populations is correlated, the reference population of the S-forwards is also likely to have a mortality improvement. From Equations (10)–(11), the hedging profits from the S-forwards will increase. As the hedging profits are equally distributed among surviving members, they could partially offset the decrease in the GSA survival payment.

In contrast, when there is an unexpected mortality increase, the survival payment will increase due to the decrease in the annuity factor and the number of survival members. Since the mortality experience between the two populations is correlated, the reference population of the S-forwards is also likely to have a mortality increase. Then the hedging profits from the S-forwards will decrease, and they could partially offset the increase in the GSA survival payment.

In either case, the position as the fixed-rate payer of the S-forwards could hedge against an unexpected mortality change in the fund population to smoothen the GSA survival payments.

Remark 3.3. In practice, due to the nature of longevity risk, annuity providers and pension funds require long-dated hedging instruments to match the duration of their liability. Short-dated hedging instruments provide limited exposure to long-term longevity risk and are mostly sensitive to short-term mortality shocks. In contrast, long-dated hedging instruments capture the cumulative survival probability over a horizon, which reflects the structure of pension and annuity liabilities. In our framework, while the S-forward contract has a fixed contractual maturity $T^* > 1$, it is closed annually through offset trading. At the beginning of each year, a new S-forward is entered into. At the end of the year, its mark-to-market value is realized through a closing offset transaction with the same maturity structure. This rolling mechanism is conceptually analogous to the dynamic management of futures contracts[9] in financial markets (Hull & Basu, 2016). This allows the fund manager to dynamically rebalance the hedge in response to evolving longevity expectations. Although the contract does not reach maturity, its value reflects the market's updated view of future survival probabilities, making it an effective tool for hedging systematic longevity risk. Several other studies use the same assumption that an active trading market for longevity-linked securities is available, for example, Zhou and Li (2017), Tang and Li (2021), and Tan et al. (2022). The assumed existence of such mark-to-market values and the ability to close positions each year is a theoretical simplification designed to evaluate the hedge's potential under perfect market conditions.

Remark 3.4. Our hedging framework is general and applies to other mortality pooling products, for example, the tontine scheme (Chen et al., 2021; Milevsky, 2014; Milevsky & Salisbury, 2015; Weinert & Gründl, 2021). Unlike the GSA fund in Equation (6), the total survival payment at time t in a tontine scheme is predetermined to make the tontine design actuarial fair. The total survival payment is equally distributed among all surviving members. As a result, the benefit per member is volatile due to the systematic longevity risk. Similarly, the fund manager of a tontine can use the dynamic hedging framework to smoothen benefits.

Since the expected return of an S-forward is non-positive, an immediate property of $B_{t+1}^{(H)}$ is given in the following proposition:

Proposition 3.5. *Under the assumption that* $G_x > 0$ *in the ACF model,*[10] *if* $h_t > 0$, *then* $\mathbb{E}_t[B_{t+1}^{(H)}] \leq \mathbb{E}_t[B_{t+1}]$; *otherwise, if* $h_t < 0$, *then* $\mathbb{E}_t[B_{t+1}^{(H)}] \geq \mathbb{E}_t[B_{t+1}]$.

[9]In this paper, we follow the literature in using the term "S-forwards" instead of "S-futures". However, they are traded as futures.

[10]This is not an unrealistic assumption. Many studies show that life expectancy has significantly improved during the past millennium, for example, Li et al. (2020). We will also confirm this assumption in our numerical study in Appendix E.

Proof. See Appendix A.2. □

We aim to identify the optimal hedging strategy over a set of admissible strategies that satisfy the following assumptions.

Definition 3.6. A triplet $\left(h_t, \mathrm{Var}_t\left[B_{t+1}^{(H)}\right], \mathbb{E}_t\left[B_{t+1}^{(H)}\right]\right)$ is called an admissible strategy at time t if

- h_t, $\mathrm{Var}_t\left[B_{t+1}^{(H)}\right]$, and $\mathbb{E}_t\left[B_{t+1}^{(H)}\right]$ are $\mathcal{F}_t$-measurable;
- h_t, $\mathrm{Var}_t\left[B_{t+1}^{(H)}\right]$, and $\mathbb{E}_t\left[B_{t+1}^{(H)}\right]$ take values in $\mathbb{R}$, $\mathbb{R}^+$, and $\mathbb{R}$, respectively.

Proposition 3.5 asserts that if GSA members hedge against the systematic longevity risk to smoothen the survival benefits, the expectation of survival benefits will decrease. In contrast, if the GSA members' objective is to increase the expectation of the survival payment, the fund can be the floating-rate payer of the S-forwards and the variance of the survival payments will increase. Thus, there is a mean-variance trade-off, which can be described by the mean-variance set in the following definition.

Definition 3.7. The mean-variance set of the hedge at time t is the collection of the tuple $(\mathrm{Var}_t[B_{t+1}^{(H)}], \mathbb{E}_t[B_{t+1}^{(H)}])$ among all admissible strategies. The global minimum variance hedging strategy achieves the GMVP on the mean-variance set, which has the minimum variance among all admissible hedging strategies.

Proposition 3.8. *Given the latest information at time t, which is $\left\{F_t^+, N_t, K_t, k_t^{(F)}, k_t^{(R)}\right\}$, the mean-variance set of the longevity hedge can be expressed as:*

$$\mathrm{Var}_t\left[B_{t+1}^{(H)}\right] = A_{1,t}\left(\mathbb{E}_t\left[B_{t+1}^{(H)}\right]\right)^2 + A_{2,t}\mathbb{E}_t\left[B_{t+1}^{(H)}\right] + A_{3,t},$$

where

$$\begin{aligned}
A_{1,t} &= \mathrm{Var}_t\left[\frac{P_{t+1}(t)}{S_{x+t,t}^{(F)}(1)}\right]\left(\mathbb{E}_t\left[\frac{P_{t+1}(t)}{S_{x+t,t}^{(F)}(1)}\right]\right)^{-2}\\
A_{2,t} &= 2(A_{4,t} - A_{1,t}\mathbb{E}_t[B_{t+1}]),\\
A_{3,t} &= \mathrm{Var}_t[B_{t+1}] - 2A_{4,t}\mathbb{E}_t[B_{t+1}] + A_{1,t}(\mathbb{E}_t[B_{t+1}])^2,\\
A_{4,t} &= \mathrm{Cov}_t\left[B_{t+1}, \frac{P_{t+1}(t)}{S_{x+t,t}^{(F)}(1)}\right]\left(\mathbb{E}_t\left[\frac{P_{t+1}(t)}{S_{x+t,t}^{(F)}(1)}\right]\right)^{-1}.
\end{aligned}$$

The GSA fund can achieve the GMVP on the mean-variance set following the global minimum variance hedging strategy:

$$h_t^{(\mathrm{GMVP})} := -\mathrm{Corr}_t\left[\frac{P_{t+1}(t)}{N_{t+1}}, B_{t+1}\right]\frac{\mathrm{Std}_t[B_{t+1}]}{\mathrm{Std}_t\left[\frac{P_{t+1}(t)}{N_{t+1}}\right]}. \tag{12}$$

Proof. See Appendix A.3. □

The global minimum variance hedging strategy in Equation (12) has the same structure as the minimum variance hedge ratio in the finance literature when the underlying asset of the hedging instrument differs from the asset to be hedged. The population basis risk has the same interpretation as the cross-hedging risk, which comes from the imperfect correlation between the two assets. As we explain in Remark 3.2, the correlation coefficient between $\frac{P_{t+1}(t)}{S^{(F)}_{x+t,t}(1)}$ and B_{t+1} is negative, so the global minimum variance hedge ratio is positive. We make the following definition in terms of the GSA members' risk preferences:

Definition 3.9. When $h_t > 0$, a longevity hedging strategy is called a risk-mitigating strategy; when $h_t < 0$, a longevity hedging strategy is called a risk-seeking strategy; when $h_t = 0$, the GSA members are risk-neutral to systematic longevity risk.

We follow Alizadeh et al. (2008) to construct a one-step ahead hedging strategy and assume that the fund manager aims to solve the following mean-variance optimization problem for the members in each step:

$$\min_{h_t\in\mathbb{R}}\left\{V_t(h_t|\mathcal{F}_t) := \mathrm{Var}_t\left[B^{(H)}_{t+1}\right] - 2\phi_t\left(\mathbb{E}_t\left[B^{(H)}_{t+1}\right] - \mathbb{E}_t[B_{t+1}]\right)\right\}, \tag{13}$$

where $V_t(h_t|\mathcal{F}_t)$ is the value function and the parameter $\phi_t(\geq 0)$ controls the mean-variance trade-off.

Remark 3.10. A one-step ahead hedging framework is suitable for our research context, as the mortality data of a whole population is usually published annually. We observe the time-varying indices $\{K_t\}$ and $\{k_t^{(i)}\}$ in the ACF model on an annual basis. However, a continuous dynamic hedging framework would require the whole population's mortality information continuously.

Remark 3.11. Alizadeh et al. (2008) propose a one-step ahead hedging strategy for energy commodities using futures based on a risk minimization objective, assuming that futures follow a martingale process. As a result, the expected returns from the hedged portfolio will not change, and the minimum variance hedge ratio is equivalent to the utility-maximizing hedge ratio (Kroner & Sultan, 1993). However, in this paper, as shown in Proposition 3.5, the expected returns from the hedged portfolio are affected by the number of S-forwards held. Therefore, we consider the utility-maximizing hedging based on the economic benefits of the members. At each rebalancing date, the mean-variance objective is related to the GSA survival benefit at the next rebalancing date. Our problem formulation is natural since the main objective of the GSA fund is to share idiosyncratic longevity risk and provide lifetime income rather than to pay a large amount of death

benefit. Note that $\mathbb{E}_t[B_{t+1}]$ is a known constant at time t and does not affect the optimal hedge ratio. In the formulation in Equation (13), we subtract the conditional mean of the unhedged benefit to better present the numerical results in Section 4.

The optimal semi-analytic solution to the mean-variance optimization problem is presented in the following proposition:

Proposition 3.12. *The optimal hedge ratio h_t^* to the optimization problem in Equation (13) is expressed as:*

$$h_t^*\left(F_t^+, N_t, K_t, k_t^{(F)}, k_t^{(R)}, \phi_t\right) = \frac{\phi_t \mathbb{E}_t\left[\frac{P_{t+1}(t)}{N_{t+1}}\right] - \mathrm{Cov}_t\left[\frac{P_{t+1}(t)}{N_{t+1}}, B_{t+1}\right]}{\mathrm{Var}_t\left[\frac{P_{t+1}(t)}{N_{t+1}}\right]}. \tag{14}$$

A necessary condition to guarantee that the hedging strategy is risk-mitigating is

$$\phi_t < \phi_t^{(RN)}\left(F_t^+, N_t, K_t, k_t^{(F)}, k_t^{(R)}\right) := A_{4,t}, \tag{15}$$

where $\phi_t^{(RN)}$ the risk-neutral (mean-variance) trade-off parameter.

Proof. See Appendix A.4. □

Remark 3.13. The semi-closed-form solution of h_t^* in Equation (14) requires Monte Carlo simulation to numerically evaluate the conditional mean, variance, and covariance at time t. From Equation (11), $P_{t+1}(t)$ is a conditional expectation at time $t+1$. Evaluating h_t^* requires the nested Monte Carlo method: first, simulate M_1 mortality paths from t to $t+1$ to evaluate B_{t+1} and N_{t+1}; second, simulate M_2 conditional mortality paths for each of the M_1 mortality paths to evaluate $P_{t+1}(t)$. The nested Monte Carlo method is computationally intensive. We use the approximation method for the spot survival probability in Cairns (2011) and Zhou and Li (2017) to avoid nested Monte Carlo and to make the dynamic hedge framework more practical. More specifically, in the second step of the nested Monte Carlo method, we directly approximate the spot survival probability at time $t+1$ to avoid further simulating the M_2 conditional mortality paths. Appendix B presents the approximation method.

By definition, $\phi_t^{(RN)}$ is determined to make a GSA member risk-neutral to the systematic longevity risk. A hypothetical member with a mean-variance trade-off parameter $\phi_t^{(RN)}$ is indifferent in hedging the systematic longevity risk or not. In the formulation of the mean-variance optimization problem in Equation (13), a large value of ϕ_t indicates that GSA members put more weight on maximizing the expectation. An individual with a mean-variance trade-off parameter $\phi_t < \phi_t^{(RN)}$ is willing to hedge the systematic longevity risk. A higher risk-neutral trade-off parameter, $\phi_t^{(RN)}$, implies a wider set of ϕ_t to yield a risk-mitigating strategy, and members are more willing to hedge longevity risk. Therefore, $\phi_t^{(RN)}$ measures the willingness of a GSA member to hedge the systematic longevity risk.

When we plot the standard deviation of $B_{t+1}^{(H)}$ on the horizontal axis and the mean on the vertical axis, the mean-variance set shows a parabolic shape as presented in Figure 4. The mean-variance set shows the mean-variance trade-off: if members are willing to hedge the systematic longevity risk to reduce the variance, the mean also decreases. The mean-variance set is closely connected to modern portfolio selection theory (Markowitz, 1952). The upper part of the mean-variance set is the efficient set, on which the fund manager chooses the optimal hedge ratio based on the GSA members' risk preferences, while the lower part represents the inefficient set. It is not optimal to select a hedging strategy on the inefficient set, since it has a lower return given the same level of risk. The dotted line is the risk-neutral line when $\phi_t = \phi_t^{(RN)}$. When members are risk-neutral, the fund manager selects the point without hedge on the efficient set, which can be viewed as the "market portfolio" in portfolio selection theory. When members are risk-averse, the fund manager will choose a positive hedge ratio (long S-forward) in the risk-averse region, which lies to the left of the risk-neutral line. In contrast, when members are risk-seeking, the fund manager will choose a negative hedge ratio (short S-forward) in the risk-seeking region, which lies to the right of the risk-neutral line. Likewise, when investors select the optimal portfolio on the capital market line, risk-averse investors invest in both risk-free assets and the market portfolio, and risk-seeking investors borrow money at the risk-free interest rate to invest in the market portfolio to achieve a higher expected return. In the longevity hedge, S-forwards play a role similar to risk-free assets in portfolio selection theory. In deriving the mean-variance set, we assume that only one S-forward is available in the capital market. It is worthwhile to consider using a different or a combination of S-forwards (with a different reference age or time-to-maturity) to achieve a better mean-variance trade-off. This is out of the scope of this paper and is left for future research.

In this paper, we assume that members are risk-averse and the mean-variance trade-off parameter is proportional to the risk-neutral trade-off parameter as:

$$\phi_t := (1 - \alpha)\phi_t^{(RN)},$$

where $0 \leq \alpha \leq 1$ is the risk-averse ratio. The risk-averse ratio measures the degree of risk-aversion of a GSA member and controls the shape of the value function, and affects the optimal

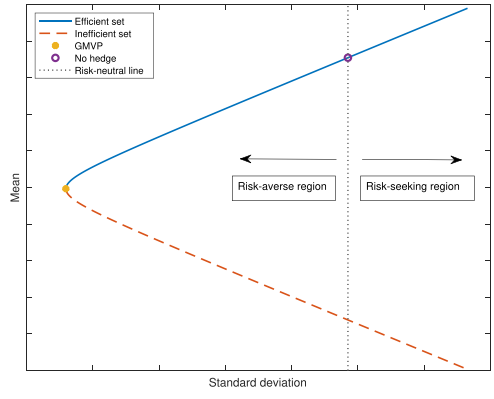

FIGURE 4 The mean-variance set of longevity hedge using S-forwards for the GSA fund members. The mean-variance set shows a parabolic shape. GSA, group self-annuities. [Color figure can be viewed at wileyonlinelibrary.com]

hedging strategy. A member with a low risk-averse ratio puts more weight on the mean in the mean-variance trade-off.

For a risk-mitigating strategy, we use the VRR, which measures the proportional reduction in the variance of the total survival benefit relative to the unhedged GSA survival benefit, to evaluate the hedge effectiveness. The VRR is defined as:

$$\mathrm{VRR}_t(\phi_t) := 1 - \frac{\mathrm{Var}_t\left[B_{t+1}^{(H)}\right]}{\mathrm{Var}_t[B_{t+1}]}, \text{ for } \phi_t < \phi_t^{(RN)}.$$

The VRR lies between zero and one, and a VRR close to one means the hedge is more effective in offsetting an unexpected mortality change in the fund population. However, since we assume that the population basis risk exists, it is generally not possible to achieve a perfect hedge with $\mathrm{VRR} = 1$.

Similarly, we use the MRR to measure the extent to which a risk-mitigating strategy reduces the expected survival benefit. The MRR is defined as:

$$\mathrm{MRR}_t(\phi_t) := 1 - \frac{\mathbb{E}_t\left[B_{t+1}^{(H)}\right]}{\mathbb{E}_t[B_{t+1}]}, \text{ for } \phi_t < \phi_t^{(RN)}.$$

The fund manager aims to find an optimal balance between the VRR and MRR, as members prefer low variability and a high level of survival benefits. On the efficient set, as the hedge ratio increases, both VRR and MRR increase. Members aim to minimize the variance term and maximize the mean term in the value function, and the optimal value function $V_t(h_t^*|\mathcal{F}_t)$ captures the optimal trade-off between the increasing VRR and MRR given their risk preference. While the value of the function may offer limited insight on its own, comparing value functions across strategies provides more meaningful information. The value function can be interpreted as a "utility function" used to select the optimal hedging strategy. For two hedging strategies, h_t^A and h_t^B, members prefer strategy h_t^A if

$$V_t\left(h_t^A|\ \mathcal{F}_t\right) - V_t\left(h_t^B|\ \mathcal{F}_t\right) < 0.$$

Members can also use the value function to decide whether to hedge or not. For a risk-mitigating strategy h_t, a decrease in the optimal value function, that is,

$$V_t(h_t|\mathcal{F}_t) - V_t(0|\mathcal{F}_t) < 0,$$

indicates that the benefit of hedging exceeds its cost and members gain from the longevity hedge.

4 | NUMERICAL RESULTS

This section provides illustrative numerical results for the dynamic longevity hedging strategy. In Section 4.1, we describe the data and model assumptions for the numerical study. Section 4.2 presents the baseline results of the longevity hedge. Section 4.3 conducts sensitivity tests to

highlight the robustness of the hedging strategy, where we change the reference age of the S-forwards, the time-to-maturity of the S-forwards, the hedger's population, the risk-free interest rate, the pool size of the GSA fund, and the assumed mortality model.

4.1 | Data and assumption

In the numerical illustrations, we assume that the fund population of the GSA portfolio (Population F) is the England and Wales total population. The reference population of the S-forwards (Population R) is the United Kingdom total population. This assumption mimics the reality that the fund population is a subset of a whole population and the choice of the two populations is similar to the setting presented in Zhou and Li (2017). Mortality rates for the two populations are assumed to follow the ACF model as presented in Section 2.1. The parameters of the ACF model are calibrated to the unisex mortality data of the two populations aged 65–99 over the period 1966 to 2021.[11,12] Mortality data are downloaded from Human Mortality Database (2024) and smoothed using the weighted penalized regression spline method provided in the `demography` package (Hyndman, 2023) in R. The smoothing step removes the jaggedness of mortality between ages and ensures that mortality is an increasing function of age in the range we consider. We use the first-order singular value decomposition method (Zhou & Li, 2017) to estimate the model parameters. The calibration of the ACF model is presented in Appendix E. The assumption in Proposition 3.5 that G_x is positive for the two populations aged 65–99 is satisfied. This is supported by the observation that the common mortality trend for the two populations is improving over time.

We consider a homogeneous GSA pool and assume that the pool size is large, implying that there is no small sample risk. The hedging horizon of the GSA fund is 35 years. In the calculation of the annuity factors in Equation (8), we assume that $m_{x,t} = m_{99,t}$ for $x \geq 100$, thus there is no systematic longevity risk after age 100. Unless otherwise stated, we use the baseline assumptions summarized in Table 1. The chosen risk loading parameter is equivalent to an annual risk premium of 0.03% reported in Tang and Li (2021), where the risk premium of S-forwards is calibrated to the market data in the UK.

4.2 | Baseline results

To illustrate the mean-variance trade-off of the longevity hedge and how the risk-averse ratio affects the optimal hedge, as an example, we present the mean-variance set and the optimal hedging strategy at time zero in Figure 5. The mean-variance trade-off parameter, ϕ_t, controls the shape of the value function, and members select the optimal hedging strategy on the efficient set that minimizes the value function. Recall that individuals with a smaller value of ϕ_t are more risk averse and care more about removing the payment variance than increasing the

[11]We performed robustness check, and the inclusion of the year 2022 (which reflects part of the COVID-affected mortality) or the exclusion of the mortality data during the COVID-19 period does not materially change the main findings of the paper. Due to space constraints, we do not include the detailed results in this section, which can be provided upon request.

[12]We set the year 2021 as the base year ($t = 0$) for all forward simulations. The time-varying indices K_t, $k_t^{(F)}$, and $k_t^{(R)}$ are calibrated using historical mortality data from 1966 to 2021.

TABLE 1 Baseline assumptions in the numerical study. The assumption of time-to-maturity of the S-forwards is the same as the assumption in Tan et al. (2022).

Age of the GSA members at the inception of the fund	x	**65**
Initial contribution per member	c	\$10,000
GSA payment frequency		Yearly[a]
Risk-free interest rate	r^f	1% per annum
Reference age of the S-forwards	x_f	75
Time-to-maturity of the S-forwards	T^*	10 years
Risk loading parameter	λ	0.3%

[a]Existing risk-pooling arrangements include the QSuper Lifetime Pension in Australia and the GuardPath Modern Tontine in Canada have an annual benefit payment frequency.

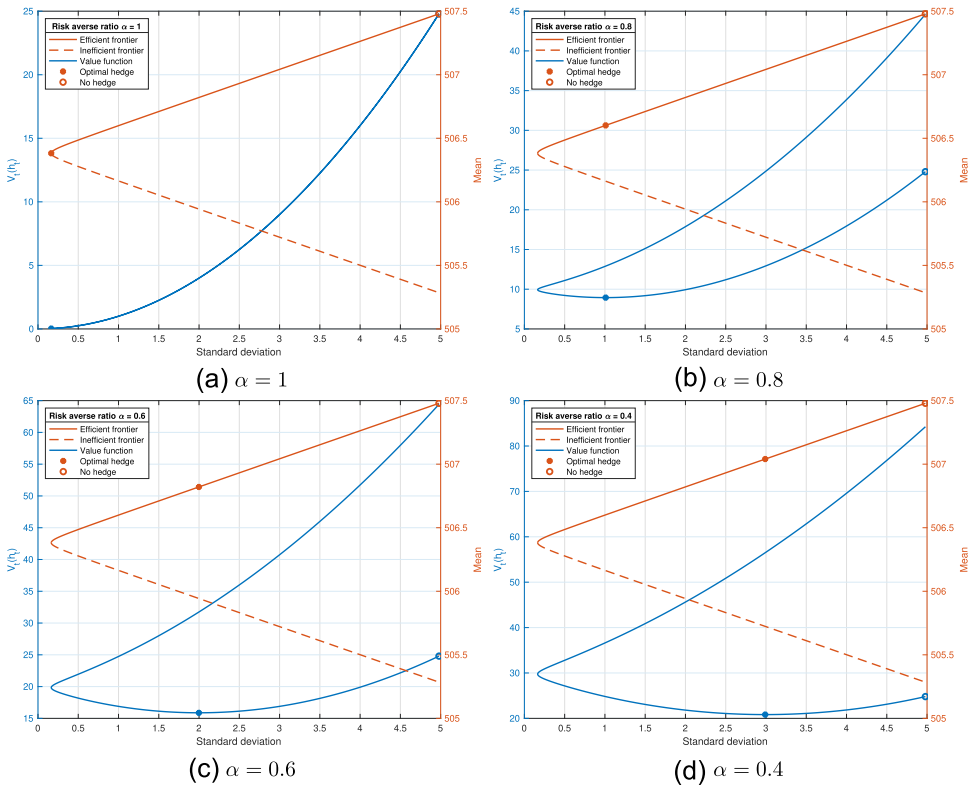

FIGURE 5 The mean-variance set and the value function at time $t = 0$ with selected values of the risk aversion parameter α. [Color figure can be viewed at wileyonlinelibrary.com]

mean of the payment. As reflected in Figure 5a, when $\alpha = 1$, members are fully risk averse and the fund manager selects the global minimum variance point (GMVP) as the optimal hedging strategy. In Panels (b)–(d), as members are less risk averse, we observe that the optimal hedging strategy moves towards the one without hedge on the efficient set. We note that the value function increases faster for a hedging strategy on the inefficient set, since given the same level of variance reduction, the hedge has a larger negative impact on the mean.

We emphasize that in Proposition 3.12, the optimal hedge ratio, h_t^*, and the risk-neutral trade-off parameter, $\phi_t^{(RN)}$, are path-dependent. The optimal solution depends on the latest information available at time t, which is $\{F_t^+, N_t, K_t, k_t^{(F)}, k_t^{(R)}\}$. A different mortality path may lead to a different optimal solution. As a result, the hedge effectiveness measurements we consider, which are VRR, MRR, and optimal value function, are also path-dependent. To compute these three metrics and quantify their uncertainty, we adopt the simulation procedures as follows:

- First, we simulate $M_1 = 20,000$ primary mortality paths for both populations.
- On each of these M_1 outer paths, we simulate $M_2 = 20,000$ conditional mortality paths and compute the path-dependent optimal hedging strategy using the numerical approximation described in Remark 3.13, which involves evaluating conditional expectations, variances, and covariances at each time point in Equation (14).
- This results in M_1 estimates for the VRR, MRR, and the optimal value function at each time point.
- We then compute 95% confidence intervals using the 2.5th and 97.5th empirical percentiles of the M_1 estimates.

We now assess the member's willingness to hedge longevity risk. An immediate observation from Figure 6 is that $\phi_t^{(RN)}$ shows a decreasing trend through time in general, indicating that GSA members are more willing to hedge the systematic longevity risk when they are younger. In Equation (8), the annuity factor is a sum of discounted survival probabilities. When members are younger, there are more terms in the summation, and the annuity factor is more sensitive to an unexpected change in the time-varying indices in the ACF model. Meanwhile, when members are younger, the hedging profits and the survival benefits are more correlated and the hedge is more effective since population basis risk increases as age increases (see Figure 7 and Table 2 in this subsection). Another observation is that $\phi_t^{(RN)}$ is a decreasing function of the death benefit payment ratio, β. When β increases, members leave less mortality credit to the fund and the survival benefit, B_t, decreases (Olivieri et al., 2022). As a result, from Equation (15) we know $\phi_t^{(RN)}$ decreases since the covariance decreases. Members are more willing to hedge longevity risk when the GSA fund pays less death benefit.

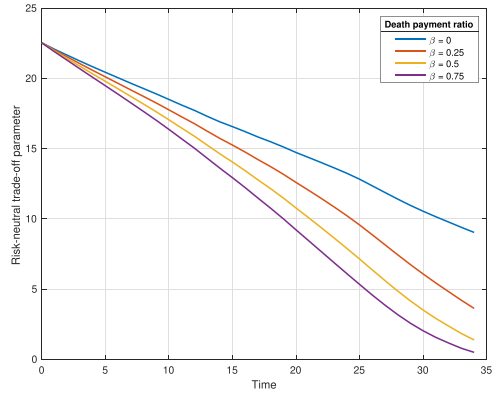

FIGURE 6 The mean of the risk-neutral trade-off parameter $\phi_t^{(RN)}$ over time. [Color figure can be viewed at wileyonlinelibrary.com]

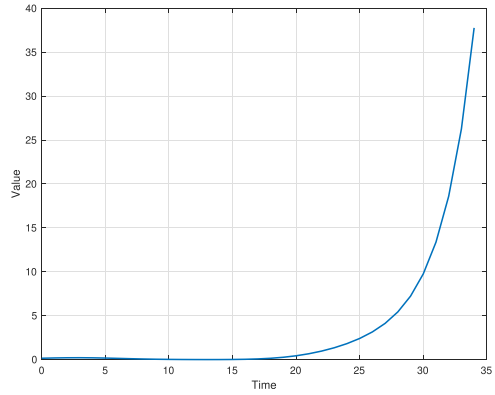

FIGURE 7 The value of the population basis risk index I_t for $t = 0, 1, ..., 34$. [Color figure can be viewed at wileyonlinelibrary.com]

TABLE 2 The variance and mean reduction ratios of the hedge at selected ages ($\alpha = 0.8$ and $\beta = 0$).

Age	Mean	Minimum	Maximum	95% confidence interval
Variance reduction ratio				
65	95.89%	95.88%	95.90%	(95.89%, 95.90%)
70	95.91%	95.88%	95.93%	(95.90%, 95.92%)
75	95.95%	95.94%	95.96%	(95.95%, 95.96%)
80	95.93%	95.92%	95.94%	(95.93%, 95.94%)
85	94.78%	93.71%	95.41%	(94.34%, 95.14%)
90	84.17%	81.76%	85.60%	(83.24%, 84.93%)
95	50.09%	45.19%	53.71%	(48.35%, 51.75%)
Mean reduction ratio				
65	0.1729%	0.1726%	0.1731%	(0.1728%, 0.1730%)
70	0.2037%	0.1918%	0.2124%	(0.1989%, 0.2083%)
75	0.2306%	0.1980%	0.2664%	(0.2146%, 0.2485%)
80	0.2617%	0.1905%	0.3678%	(0.2247%, 0.3059%)
85	0.2913%	0.1934%	0.4402%	(0.2391%, 0.3530%)
90	0.2943%	0.1630%	0.5773%	(0.2213%, 0.3894%)
95	0.2678%	0.1461%	0.3992%	(0.2136%, 0.3251%)

To measure how the longevity hedge can reduce the variance of the GSA survival benefits, we show the VRR in Table 2 where we assume that the risk-averse ratio $\alpha = 0.8$ and the death benefit payment ratio $\beta = 0$. The hedge is very effective in reducing the variance of the GSA survival benefit by more than 90% on average in the first 20 years, and by more than 50% on average in the following 10 years. In addition, in the first 20 years, the minimum VRR is greater than 90% and the 95% confidence intervals are very tight. However, the hedge is less effective

when members are older. As shown in Appendix E, as age increases, the shape parameter G_x decreases, while the shape parameters $g_x^{(i)}$ reflect an increasing trend. As a result, the population basis index I_t increases as age increases, as reflected in Figure 7, and the population basis risk plays an increasingly important role in the hedge. Mortality for the older population is less sensitive to the common time-varying index K_t. Then the hedging profit or loss $\frac{P_{t+1}(t)}{N_{t+1}}$ and the survival benefit B_{t+1} are less correlated and the hedge is less effective in smoothening the GSA survival benefit. Since a longevity hedge reduces the mean of the survival benefit, Table 2 also reports the MRR to help members assess the impact. As age increases, the MRR first increases then decreases, with its magnitude broadly aligning with the risk loading charged on the S-forwards. From Equation (10), the MRR can be expressed as:

$$\mathrm{MRR}_t(\phi_t) = -\frac{h_t \mathbb{E}_t\left[\frac{P_{t+1}(t)}{N_{t+1}}\right]}{\mathbb{E}_t[B_{t+1}]}, \text{ for } \phi_t < \phi_t^{(RN)}.$$

In this equation, h_t decreases and $\mathbb{E}_t[B_{t+1}]$ increases over time. Meanwhile, since the number of surviving members N_{t+1} decreases, $\mathbb{E}_t\left[\frac{P_{t+1}(t)}{N_{t+1}}\right]$ increases. As a result, MRR_t exhibits concavity over time.

As reflected in Table 2, the hedge reduces both the mean and variance of the survival benefit, as indicated by the positive values of VRR and MRR. Given this trade-off, members are naturally concerned with whether the benefit of hedging outweighs its cost. To evaluate this, we compare the optimal value function against the benchmark case without hedging. We highlight that a decrease in the optimal value function indicates that the benefit of hedging exceeds its cost. Table 3 shows the optimal value function with and without hedge when $\alpha = 0.8$ and $\beta = 0$. We observe that the hedge reduces the optimal value function significantly. It decreases by 63.93%, 63.94%, 63.97%, 63.95%, 63.17%, 56.05%, and 33.05%, at ages 65, 70, 75, 80, 85, 90, and 95, respectively. This confirms that the benefit of variance reduction exceeds the cost of reduction in the mean. Meanwhile, when members are younger, the hedge is more effective and they benefit more from the hedge. Appendix C presents the hedging results when the S-forwards are fairly priced. The key finding is that the risk premium mainly increases MRR and has a minimal effect on VRR.

Figure 8 presents how the risk-averse ratio, α, impacts the optimal hedge ratio, h_t^*, the VRR, the MRR, and the optimal value function. In this figure, we show the mean curves and assume that the death benefit payment ratio, $\beta = 0$. The optimal hedge ratio exhibits an increasing pattern as α increases. As the members are more risk-averse, they are more interested in reducing the variance rather than increasing the mean in the optimization problem. Consequently, the fund manager will use more S-forwards to hedge longevity risk and the hedge is more effective in reducing the payment variance. However, as shown in Panel (c), the negative effect of the benefit increases as members become more risk averse and use more S-forwards. In Panel (d), the dashed and solid lines represent the value function without and with hedge, respectively. We observe that the optimal value function decreases with the dynamic hedge. The optimal value function exhibits a decreasing pattern as α increases. This confirms that in our numerical example, for the risk-mitigating strategies, as the hedge ratio increases, the reduction in variance dominates the decrease in mean. Fixing the risk-averse ratio, the optimal value function grows faster and is closer to the benchmark line without hedge in the last 10 years. This is because the longevity hedging strategy is less effective in reducing the variance in the last 10 years and members benefit less from the hedge.

TABLE 3 The impact of longevity hedge on the optimal value function at selected ages ($\alpha = 0.8$ and $\beta = 0$).

Age	Mean	Minimum	Maximum	95% confidence interval
Optimal longevity hedge				
65	8.92	8.41	9.49	(8.67, 9.17)
70	9.40	5.15	18.77	(6.88, 12.55)
75	9.50	4.21	26.68	(6.09, 14.24)
80	9.58	4.10	24.37	(6.26, 14.13)
85	9.76	5.45	19.63	(7.18, 13.16)
90	12.63	3.89	43.67	(7.20, 21.05)
95	27.31	9.76	98.35	(16.12, 44.58)
Without longevity hedge				
65	24.73	23.32	26.32	(24.05, 25.42)
70	26.06	14.28	52.04	(19.09, 34.81)
75	26.38	11.67	74.02	(16.91, 39.52)
80	26.59	11.37	67.59	(17.37, 39.21)
85	26.49	14.98	52.32	(19.63, 35.47)
90	28.74	8.95	96.75	(16.52, 47.43)
95	40.98	14.21	140.76	(24.19, 66.36)

Figure 9 presents the benefits profile under two mortality path simulations, assuming $\alpha = 0.8$ and $\beta = 0$. The benefits B_{t+1} and $B_{t+1}^{(H)}$ are calculated one step ahead by fixing F_t^*, N_t, K_t, $k_t^{(F)}$, and $k_t^{(R)}$ at time t. As a result, the reported confidence intervals reflect one-step-ahead uncertainty rather than uncertainty from time zero. The results show that the hedge has a limited effect on the mean benefit, as indicated by the small MRR in Figure 8c. However, the 95% confidence intervals for $B_{t+1}^{(H)}$ are noticeably narrower than those for B_{t+1}, especially during the first 25 years, confirming the hedge's effectiveness in stabilizing benefit payments.

4.3 | Robustness of the hedging strategy

This subsection conducts sensitivity tests to check the robustness of the dynamic hedging strategy. In the sensitivity tests, we keep the risk-averse ratio and the death benefit payment ratio fixed at $\alpha = 1$ and $\beta = 0$, respectively. We repeat the experiments in Section 4.2 under alternative scenarios. In this subsection, all plots represent the mean value over time.

4.3.1 | Robustness to S-forwards' reference age and time-to-maturity

In the baseline results, we present the effectiveness of the hedging strategy based on the 10-year S-forwards referenced to the Population H aged 75. However, an S-forward with a certain

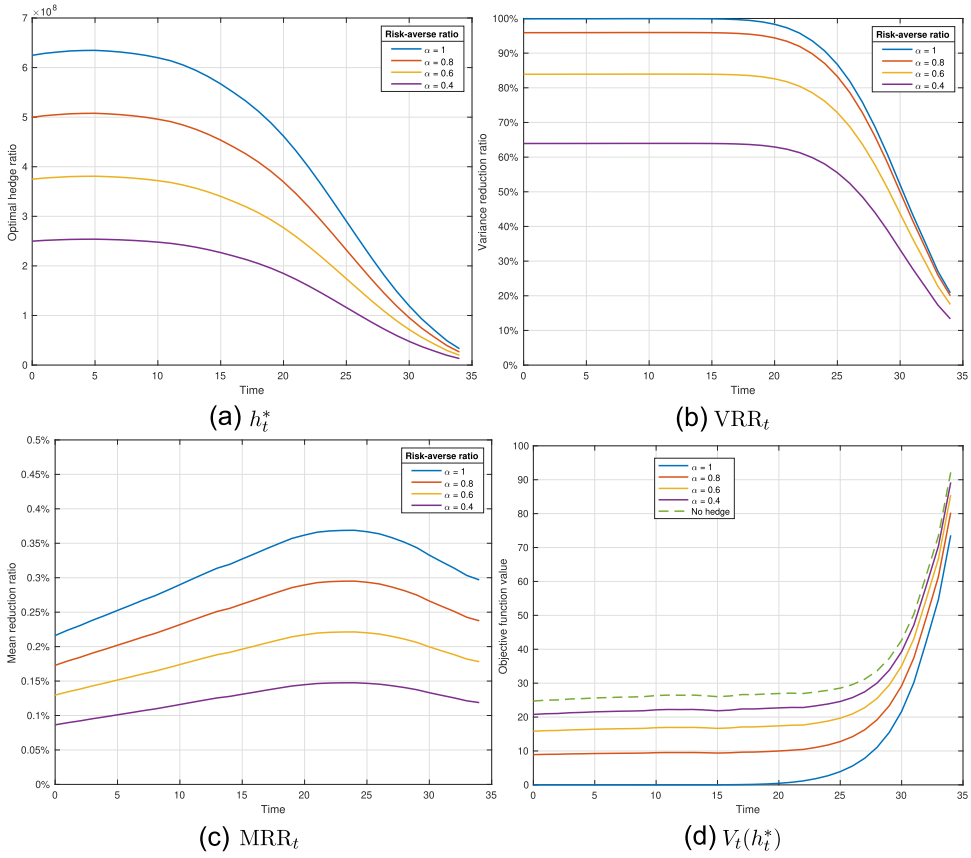

FIGURE 8 The impact of risk-averse ratio α on the optimal hedge ratio h_t^*, the VRR, the MRR, and $V_t(h_t^*)$, where we assume that $\beta = 0$. All curves represent the mean value. [Color figure can be viewed at wileyonlinelibrary.com]

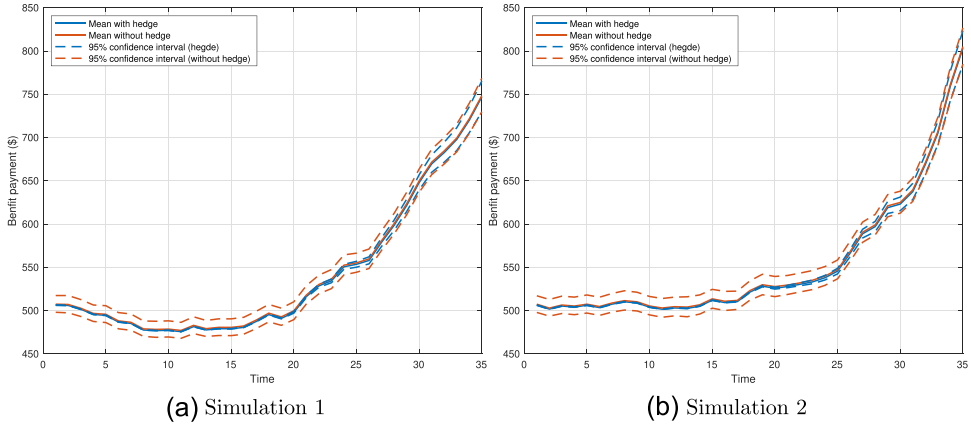

FIGURE 9 Survival benefit per member given two simulations of the mortality path. The solid and dashed lines represent the mean and 95% confidence interval, respectively. The initial contribution per member is $10,000. [Color figure can be viewed at wileyonlinelibrary.com]

reference age and time-to-maturity may not be actively traded in the market. It is worthwhile to check the robustness of the hedging strategy with a different reference age and time-to-maturity of the S-forwards.

To perform the analysis, we first fix the reference age at 75 and vary the time-to-maturity of the S-forwards by $T^* = 1, 4, 8, 12$ years. Figure 10 presents the simulation results with different maturities. We find that the longevity hedge remains effective for $T^* = 4, 8, 12$ years, indicating the robustness of the hedging strategy to the time-to-maturity of the S-forwards. In contrast, 1-year S-forwards are significantly less effective, since the VRR is smaller and decreases to near zero over time. This is because each S-forward covers only a 1-year window, whereas longevity risk persists over a multi-year horizon. Mortality trends between the fund and reference populations are more correlated over longer horizons, while short-term fluctuations introduce more basis risk over shorter horizons. A hedging instrument that focuses only 1 year ahead fails to capture the long-term nature of the systematic longevity risk. Therefore, longer-dated S-forwards provide a more stable and effective hedge by covering risk over an extended period. This result motivates the use of longer-dated S-forwards and the adoption of offset trading to close S-forward positions at year-end under the yearly rolling hedging strategy (see Remark 3.3).

We then fix the time-to-maturity at 10 years and vary the reference age of the S-forwards by $x_f = 65, 70, 85, 90$. Figure 11 depicts the simulation results with different reference ages, where the observations are similar as in Figure 10. The results demonstrate that the dynamic hedging strategy is quite robust to the S-forwards' reference age. However, when the reference age of the

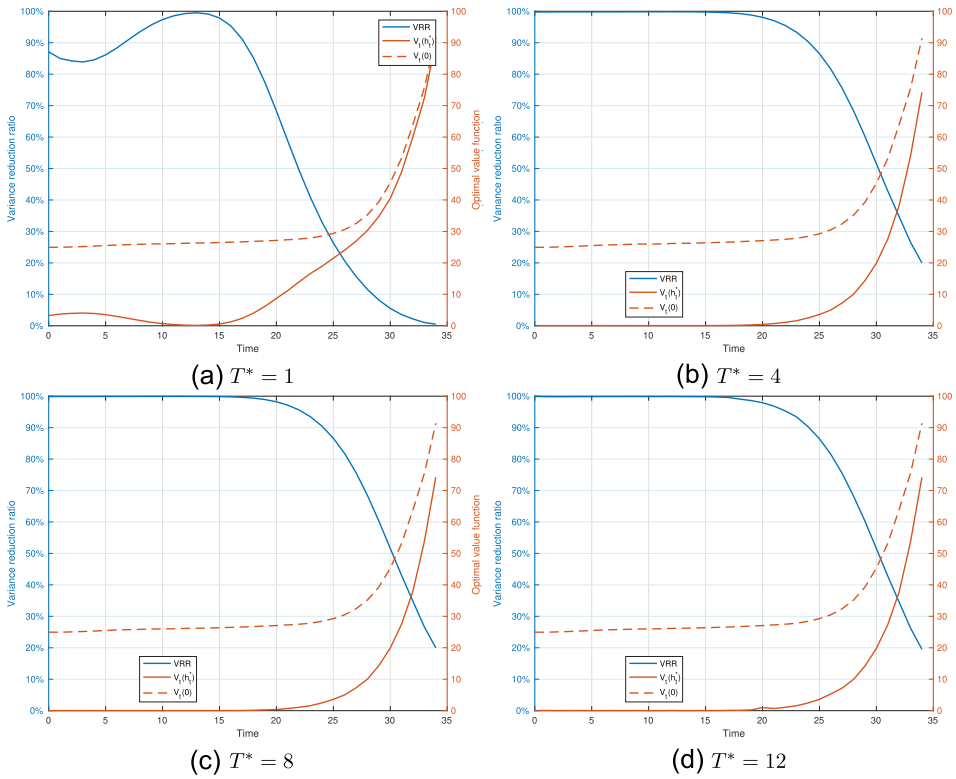

FIGURE 10 The impact of time-to-maturity on hedge effectiveness for $T^* = 1, 4, 8, 12$ years. The reference age $x_f = 75$ is kept fixed. [Color figure can be viewed at wileyonlinelibrary.com]

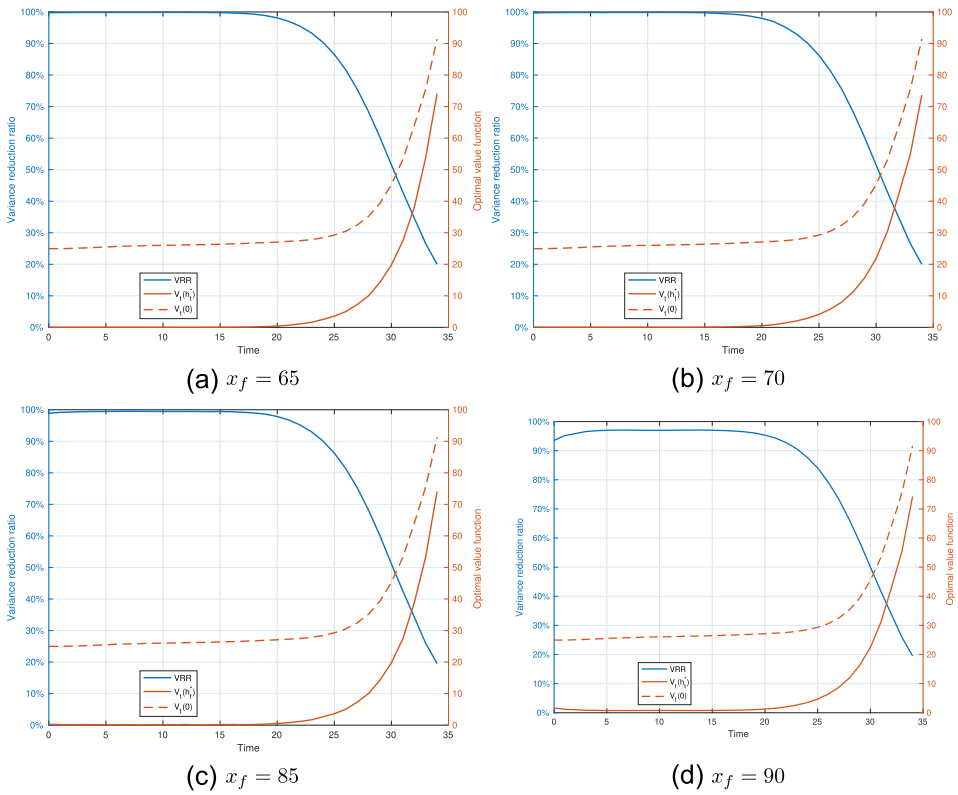

FIGURE 11 The impact of reference age on hedge effectiveness for $x_f = 65, 70, 85, 90$. The time-to-maturity $T^* = 10$ years is kept fixed. [Color figure can be viewed at wileyonlinelibrary.com]

S-forwards is 90, the hedge becomes relatively less effective, as indicated by a lower VRR in Panel (d) compared to the other cases. This is because the population basis risk index I_t increases exponentially at older ages, as shown in Figure 7, leading to a weaker correlation between the mortality of the reference population and that of the fund population. As such, the basis risk between two populations becomes more pronounced, limiting the effectiveness of S-forwards. This highlights that the S-forwards indexed to a population aged below 85 is pivotal in the longevity hedging capital market.[13] We leave hedging at very high ages for future research.

4.3.2 | Robustness to hedger's population

In the baseline results, the book population (Population F) is the England and Wales total population. Figure 12 shows the hedging results when the book population comes from other parts of the UK (Northern Ireland or Scotland). The S-forwards in the hedge are indexed to the UK total population aged 75 with a 10-year time-to-maturity. We observe that the VRR ranges from 99% to 75% in the first 25 years. In addition, the optimal value function is consistently

[13]Similarly, in hedging longevity risk for a defined benefit pension provider, Zhou and Li (2017) report that the longevity hedge is less effective when the reference age of the q-forwards is over 80.

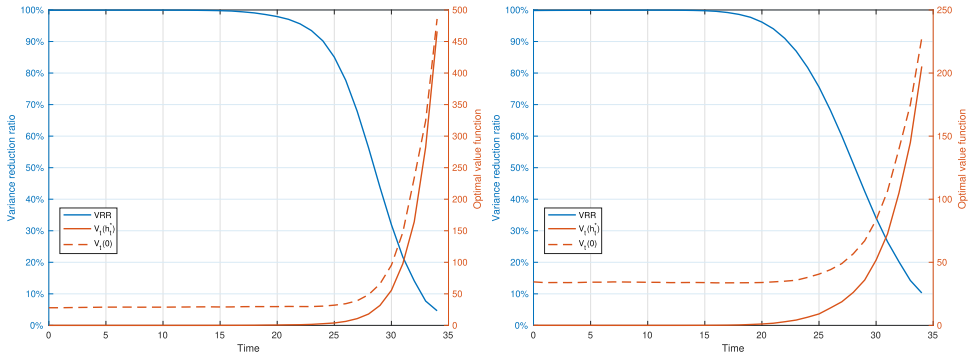

(a) Northern Ireland (b) Scotland

FIGURE 12 The impact of hedger's population on hedge effectiveness for the book population being the Northern Ireland population or the Scotland population. The time-to-maturity $T^* = 10$ years and the reference age $x_f = 75$ are kept fixed. [Color figure can be viewed at wileyonlinelibrary.com]

smaller than the benchmark. The results highlight that the standardized longevity-linked security referenced to a nationwide population is effective in hedging longevity risk for large GSA funds.

4.3.3 | Robustness to interest rate risk

The GSA fund is naturally long-dated with interest rate uncertainty being a key source of risk. For shorter maturities in practice, interest rate risk is managed independently using interest rate derivatives, such as interest rate swaps. This subsection quantifies how interest rate risk affects the effectiveness of the longevity hedge. In the analysis, we assume that the optimal hedge ratio is derived under the assumption that $r^f = 1\%$, but the realized interest rate is not the same as the assumption. More specifically, we investigate hedge effectiveness under the following two scenarios:

- Scenario 1: The realized risk-free interest rate is 0.1%, which is lower than the assumption.
- Scenario 2: The realized risk-free interest rate is 3%, which is higher than the assumption.

Figure 13 confirms that the hedge remains quite effective when the realized interest rate differs from the assumption within an absolute value of 2%, as the VRR is greater than 90% in the first 20 years. Comparing the two panels, we observe that when the realized risk-free interest rate decreases, the hedge is relatively more effective as the VRR is larger. From Equation (8), the annuity factor is more sensitive to a mortality change when the risk-free interest rate is lower. Consequently, survival payments and the profit or loss from the S-forwards are more correlated, and the longevity hedge becomes more effective. Moreover, in the last 5 years, when the realized risk-free interest rate increases, the optimal value function is closer to the benchmark line. Following an increase in the risk-free interest rate, the investment return increases, which amplifies the benefit level and variance and makes the hedge less effective.

It is worth mentioning that interest rate risk is not a major concern for the proposed dynamic hedging framework. First, it can be hedged directly using an interest rate swap. Second, risk-free interest rate adjustment is generally a slow process, and the dynamic hedging framework is effective within a 2% (absolute) change in the risk-free interest rate. Unless some extreme events occur and the risk-free interest rate changes sharply, the hedge

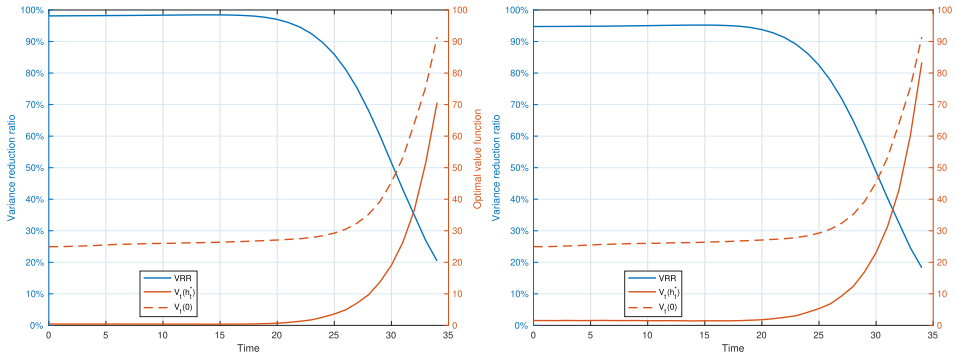

(a) Realised risk-free interest rate is 0.1% (b) Realised risk-free interest rate is 3%

FIGURE 13 The impact of interest rate risk on hedge effectiveness for a 0.1% or 3% realized interest rate. The time-to-maturity $T^* = 10$ years, the reference age $x_f = 75$, and the book population are kept fixed. [Color figure can be viewed at wileyonlinelibrary.com]

remains effective even when the hedger mis-specifies the risk-free interest rate. Third, GSA members can include the latest information on the risk-free interest rate to determine the optimal hedge ratio for the next period thanks to the dynamic hedging mechanism.

4.3.4 | Robustness to pool size

In this subsection, we bring the small sample risk in the GSA pool. When the pool size is finite, the realized mortality rate of the GSA pool may be different from its expectation and at time $t-1$, the number of survival members at the end of the period follows a binomial distribution:

$$N_t \sim \text{Binomial}\left(N_{t-1}, S^{(F)}_{x+t-1,t-1}(1)\right).$$

In computing the optimal hedge ratio, the fund manager needs to account for the additional source of uncertainty in the number of survival members.

From Figure 14, we observe that as N_0 decreases, the variance reduction decreases and the hedge becomes less effective. This is due to the increase in the idiosyncratic mortality risk in the GSA pool, and the hedging strategy is not designed for hedging the idiosyncratic mortality risk. The findings align with Li and Hardy (2011) and Zhou and Li (2017), where longevity hedging strategies for an annuity portfolio become less effective when the sample size decreases. The impact of the small sample risk becomes material when the initial pool size is less than 3000 and the VRRs are less than 90%. We highlight that even with a small initial number of members, like 3000, the hedge can reduce the payment variance by 70%–95% in the first 20 years, indicating that a significant portion of the longevity risk is removed.

4.3.5 | Robustness to model risk

In our context, model risk refers to the potential reduction in hedge effectiveness resulting from using an inaccurate mortality model to determine the optimal hedging strategy. To illustrate

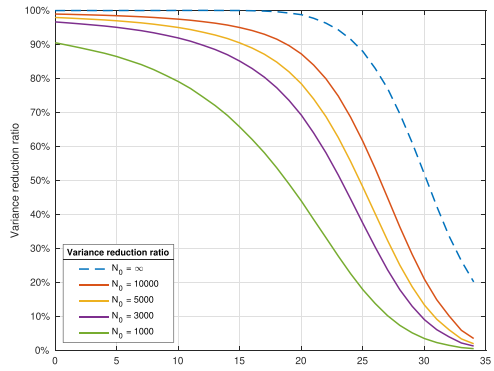

FIGURE 14 The impact of pool size on hedge effectiveness for a finite pool size with $N_0 = 10{,}000$, 5000, 3000, and 1000. The dashed line represents the case with no small sample risk. [Color figure can be viewed at wileyonlinelibrary.com]

this, we examine the effectiveness of the hedging strategy when the "true" mortality model differs from the "assumed" model, which is the ACF model. Specifically, we consider the following two alternative "true" models, and assume that the fund manager selects the optimal hedging strategy using the "assumed" model.

- Model 1: The multi-population Lee-Carter (M-LC) model (Cairns et al., 2011). In the M-LC model, the mortality rate of Population i is specified as:

$$\log\left(m_{x,t}^{(i)}\right) = a_x^{(i)} + G_x k_t^{(i)} + \epsilon_{x,t}^{(i)},$$

  where $a_x^{(i)}$ and $\epsilon_{x,t}^{(i)}$ have the same interpretation as in the ACF model. However, the two populations share the same shape parameter G_x in the M-LC model. We assume that the reference population is the dominant population and that $k_t^{(R)}$ follows a random walk with drift. The fund population is linked to the reference population through the assumption that the difference $k_t^{(R)} - k_t^{(F)}$ follows a first-order autoregressive process.

- Model 2: The multi-population Cairns–Blake–Dowd (M-CBD) model (Li et al., 2015). In the M-CBD model, the 1-year death of Population i is expressed as:

$$\log\left(\frac{q_{x,t}^{(i)}}{1 - q_{x,t}^{(i)}}\right) = k_{1,t}^{*} + k_{2,t}^{*}(x - \bar{x}) + k_{1,t}^{(i)} + k_{2,t}^{(i)}(x - \bar{x}) + \epsilon_{x,t}^{(i)},$$

  where $k_{1,t}^{*}$ and $k_{2,t}^{*}$ are common time-varying indices, $k_{1,t}^{(i)}$ and $k_{2,t}^{(i)}$ are population-specific time-varying indices, $\bar{x}$ is the average age in the data, and $\epsilon_{x,t}^{(i)}$ is an error term. The common time-varying indices follow a bivariate random walk with drift, while each population-specific time-varying index follows a first-order autoregressive process.

We implement the following procedures to determine the hedge effectiveness:

- Simulate 20,000 mortality paths using the "true" model.

- Calibrate the "assumed" model based on the simulated mortality realizations.
- Determine the optimal hedging strategy using Equation (14).
- Calculate the VRR.

Table 4 shows that the VRRs are very similar across different models. This highlights that the hedge remains effective even when the actual mortality model differs from the one used by the fund manager. The robustness of the dynamic hedging strategy suggests that the correlation between the two populations' mortality trends is not highly sensitive to the choice of mortality model. In particular, when the two populations are strongly correlated, especially within the age group 65–85, their mortality rates tend to move together in the same direction regardless of the chosen model. Furthermore, the dynamic hedging strategy can adapt to changing conditions, and regular rebalancing helps correct for deviations, further improving its effectiveness. This confirms and clarifies why the dynamic hedging strategy is immune to model risk to a large extent.

5 | GENERALIZATION TO HEDGING INVESTMENT RISK

The dynamic hedging framework above assumes that the GSA fund is fully invested in a risk-free bank account. Naturally, one might question whether the fund can manage investment risk and longevity holistically. This section aims to address this question.

To effectively manage the investment risk, the fund manager can employ a target volatility investment strategy (Doan et al., 2018; Li et al., 2022; Olivieri et al., 2022). We assume that risk management is performed sequentially, that is, the fund manager first sets a target volatility for the investment risk, then hedges the systematic longevity risk. As highlighted in Section 1, retirees prefer stable and sustained living benefits. The first step aims to enhance survival benefits by implementing a target volatility strategy for enhancing the performance of the underlying GSA fund. The second step aims to decrease the variance of survival benefits and make them smoother.

5.1 | The equity model

Let Y_t be the stock price at time t and assume that this evolves according to the Heston stochastic volatility model (Heston, 1993):

TABLE 4 The impact of model risk on the VRR at selected ages. The time-to-maturity $T^* = 10$ years, the reference age $x_f = 75$, and the book population are kept fixed. All figures represent the mean value.

Age	ACF	M-LC	M-CBD
65	99.88969%	99.88973%	99.88969%
70	99.90976%	99.91032%	99.90970%
75	99.94974%	99.95079%	99.94982%
80	99.92749%	99.92860%	99.92767%
85	98.75706%	98.72143%	98.74373%
90	88.00431%	87.66947%	87.95813%
95	53.11209%	52.18132%	53.03698%

$$dY_t = \mu Y_t dt + \delta\sqrt{v_t} Y_t dW_t^1 + \sqrt{1-\delta^2}\sqrt{v_t} Y_t dW_t^2,$$
$$dv_t = \kappa_v(\theta_v - v_t)dt + \sigma_v\sqrt{v_t} Y_t dW_t^1,$$

where μ and v_t are the instantaneous return and variance of Y_t, and W_t^1 and W_t^2 are two independent standard Brownian motions. In the Heston stochastic volatility model, the instantaneous variance v_t follows a mean-reverting process, where θ_v is the long-term mean, κ_v is the speed of mean reversion, and σ_v is the volatility. We require $2\kappa_v\theta_v \geq \sigma_v^2$ to guarantee v_t is positive (Feller, 1951). Here, δ is the correlation between the stock price and variance processes.

5.2 | Target volatility strategy

Several target volatility strategies have been proposed in literature (Doan et al., 2018; Li et al., 2022; Olivieri et al., 2022) in response to the empirically observed low-volatility anomaly: stock return and volatility processes have a negative relationship[14] (Ang et al., 2006). A low market volatility environment is associated with a high market return, and the fund increases market exposure. In contrast, a high market volatility environment is associated with a low market return, and the fund decreases market exposure. The target volatility strategy sets a target volatility for the fund. The fund manager forecasts market volatility and rebalances the investment portfolio to maintain the volatility target. The market exposure at time t, w_t, is determined as:

$$w_t = \min\left\{\frac{\mathrm{TV}}{\hat{\sigma}_t}, 1\right\},$$

where TV is the target volatility and $\hat{\sigma}_t$ is the volatility estimate at time t. The fund manager determines $\hat{\sigma}_t$ from historical observations. In particular, this is determined by the exponentially weighted moving average of the volatility (Olivieri et al., 2022):

$$\hat{\sigma}_{t+\Delta t}^2 = \eta\hat{\sigma}_t^2 + \frac{1-\eta}{\Delta t}(\log(Y_{t+\Delta t}) - \log(Y_t))^2,$$

where η is the rate of decay and $t + \Delta t$ is the next rebalancing date. In Section 5.3, we consider a weekly rebalancing frequency ($\Delta t = \frac{1}{52}$) and discretise the Heston stochastic volatility model with a weekly time increment to implement the target volatility strategy.

Depending on the investment portfolio, the target volatility strategies can be classified into two types:

[14]The inverse relationship between market volatility and expected returns can be attributed to the volatility feedback effect in models where volatility is priced (Bekaert & Wu, 2000; Wu, 2001). According to this effect, an increase in expected volatility increases the required risk premium. As investors anticipate higher compensation for bearing additional risk, this leads to a drop in current asset prices and lower returns. In contrast, a decline in expected volatility lowers the required premium and increases asset prices, resulting in higher returns.

- Type A (Olivieri et al., 2022): The fund allocates a proportion w_t into equity and $1 - w_t$ into risk-free bank account.
- Type B (Doan et al., 2018; Li et al., 2022): The fund invests fully in equity and allocates another proportion $w_t - 1$ into the futures on equity.

Proposition 5.1. *Assuming no market transaction costs, the two target volatility strategies proposed in (Olivieri et al., 2022) and (Doan et al., 2018; Li et al., 2022) are equivalent.*

Proof. See Appendix A.5. □

We use the return per unit of risk, π_t, which is expressed as:

$$\pi_t = \frac{\mathbb{E}_0[B_t]}{\mathrm{Std}_0[B_t]},$$

to measure the effectiveness of an investment strategy (Doan et al., 2018). A higher π_t means that an investment strategy is more effective. Since investment return and mortality are both stochastic processes, they contribute to the variability of benefits. Let LONG_t and INV_t denote the systematic longevity risk component and the investment risk component, respectively. Since we assume that longevity and investment risks are independent, the total variance can be decomposed as:

$$\mathrm{Var}_t[B_{t+1}] = \mathrm{LONG}_t + \mathrm{INV}_t.$$

The risk decomposition method presented in Appendix D enables us to quantify the contributions of equity and longevity risks in this equation. Due to the independence of the two risks, the total variance reduction only comes from the dynamic hedging strategy. The VRR of the dynamic hedging strategy is defined as:

$$\mathrm{VRR}_t(\phi_t) := \frac{\mathrm{Var}_t[B_{t+1}] - \mathrm{Var}_t\left[B_{t+1}^{(H)}\right]}{\mathrm{LONG}_t}, \text{ for } \phi_t < \phi_t^{(RN)}.$$

The other longevity hedging calculations in Section 3 remain the same.

5.3 | Numerical illustrations

In the numerical illustrations, we use the set of parameters in Table 5 for the Heston stochastic volatility model and consider a weekly rebalancing frequency for the target volatility strategy, while the dynamic longevity risk hedging strategy is annually rebalanced. We adopt a weekly rebalancing frequency for the target volatility strategy because the stock market is more liquid and supports more frequent trading. The other parameters are the same as those in Table 1. The volatility target is equal to the volatility multiplier times the long-term mean of volatility, $\sqrt{\theta_v}$. To show the risk decomposition, as an example,

TABLE 5 Baseline assumptions of the Heston stochastic volatility model, where we use the same set of parameters as presented in Olivieri et al. (2022).

Instantaneous return of the stock	μ	0.0849
Speed of mean reversion	κ_v	2
Long-term mean of stock variance	θ_v	0.0299
Volatility of stock variance	σ_v	0.2
Correlation between stock and variance processes	δ	−0.4480
Rate of decay in volatility forecasting	η	0.8

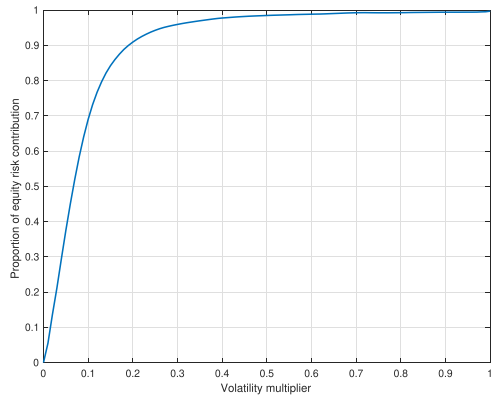

FIGURE 15 The proportion of investment risk contribution at time $t = 1$ with death benefit payment ratio $\beta = 0$. [Color figure can be viewed at wileyonlinelibrary.com]

we present the proportion of investment risk contribution at time one in Figure 15. Since the longevity risk component is fixed, the proportion of investment risk contribution increases as the volatility target increases. We have conducted a robustness check of the dynamic hedging strategy regarding the choice of target volatility. The key findings in Section 4 remain the same. Due to space constraints, we do not include detailed results of the robustness check in this subsection.

Table 6 compares the return per unit of risk for the holistic management strategy, pure target volatility (dynamic) strategy, and pure static investment strategy. The holistic strategy manages longevity risk and investment risk together. To make a fair comparison, the static investment strategy allocates a fixed proportion, which equals the volatility multiplier, into the equity and the rest into the risk-free bank account. We observe that the dynamic investment strategy performs better than the static investment strategy in terms of the return per unit of risk. The return per unit of risk decreases as the volatility multiplier increases. This is because the fund return appreciates slower relative to the volatility, consistent with the findings in Doan et al. (2018). When the fund jointly manages the investment and longevity risks (holistic approach), the return per unit of risk increases since the longevity risk component can be effectively removed through the dynamic hedge.

TABLE 6 Return per unit of risk (π_t) at selected ages for different volatility targets with risk-averse ratio $\alpha = 1$ and death benefit ratio $\beta = 0$.

Age	75			80			85		
Multiplier	Holistic	Dynamic	Static	Holistic	Dynamic	Static	Holistic	Dynamic	Static
0.1	16.9801	16.9292	16.7084	13.4847	13.4442	13.2699	11.2608	11.2270	11.1032
0.3	6.4686	6.4492	6.3675	5.1337	5.1183	5.0661	4.3880	4.3748	4.3305
0.5	3.9130	3.9013	3.8403	3.1088	3.0994	3.0633	2.6227	2.6148	2.5932
0.7	2.8781	2.8694	2.7460	2.2578	2.2511	2.1577	1.9015	1.8958	1.8180
0.9	2.3677	2.3606	2.0907	1.8494	1.8438	1.6168	1.5479	1.5432	1.3488

6 | CONCLUSION

This paper presents a novel dynamic hedging framework of systematic longevity and investment risk for GSAs. To hedge longevity risk, we use a multi-population mortality model (Li & Lee, 2005) to allow for the population basis risk. The hedging instrument we consider is a standardized longevity-linked security, namely, the S-forward. Unlike continuous-time dynamic hedging, our approach involves less frequent portfolio rebalancing, making it more practical for implementation. In addition, the framework can be extended to other longevity pooling products. Investment risk is managed using a target volatility strategy, which enhances fund performance by leveraging the negative correlation between stock prices and variance.

For longevity risk hedging, we establish a mean-variance trade-off for GSA participants and derive semi-closed-form solutions for the mean-variance set and optimal hedge ratio. To improve computational efficiency and avoid nested Monte Carlo simulations, we approximate the spot survival probabilities following Cairns (2011). Numerical studies reveal that the GSA fund contains more systematic longevity risk when members are younger or the fund pays lower death benefits. Implementing the hedging strategy significantly reduces the payment variance and increases the effectiveness of GSAs in preserving smooth income after retirement. Meanwhile, the proposed holistic approach, which manages longevity and investment risks jointly, further enhances survival payments and makes the risk-pooling scheme more appealing. The proposed hedging strategy is robust across different S-forward reference ages, maturities, book populations, interest rate risks, GSA pool sizes, and model risk.

Our study focuses on the mean-variance trade-off, with the minimum variance hedge ratio emerging as a special case when the trade-off parameter is zero. Future research could explore alternative hedging objectives, such as maximizing the Sharpe ratio (Howard & D'Antonio, 1984; Sharpe, 1994) or minimizing downside risk (Fishburn, 1977; Roy, 1952). While we assume the availability of a single S-forward, future extensions could consider dynamically trading multiple S-forwards to achieve a better mean-variance trade-off. Additionally, as population basis risk increases with age, hedging becomes less effective for older members. Future work can investigate strategies to mitigate the residual systematic longevity risk within the GSA pool.

Finally, we emphasize that the pool size is not the only source of the idiosyncratic mortality risk. Factors such as individual health and functional disability status play significant roles. For example, Kabuche et al. (2024) propose a GSA scheme that shares mortality risk across multiple

health states. A promising research direction would be to explore hedging strategies for GSAs that incorporate individual health or functional disability risks.

ACKNOWLEDGMENTS

The authors thank two referees for helpful comments and suggestions, which have helped improve the quality of the paper. This study was partly supported by the Australian Research Council (DP250102415, DP210101195, and DE200101266). Open access publishing facilitated by University of New South Wales, as part of the Wiley - University of New South Wales agreement via the Council of Australian University Librarians.

CONFLICT OF INTEREST STATEMENT

The authors declare no conflicts of interest.

DATA AVAILABILITY STATEMENT

The data that support the findings of this study are openly available in the Human Mortality Database at https://www.mortality.org/.

ORCID

Yawei Wang https://orcid.org/0000-0001-7587-4149

REFERENCES

Alizadeh, A. H, Nomikos, N. K., & Pouliasis, P. K. (2008). A Markov regime switching approach for hedging energy commodities. *Journal of Banking and Finance*, *32*(9), 1970–1983.

Ang, A., Hodrick, R. J., Xing, Y., & Zhang, X. (2006). The cross-section of volatility and expected returns. *The Journal of Finance*, *61*(1), 259–299.

Bégin, J., & Sanders, B. (2024). Benefit volatility-targeting strategies in lifetime pension pools. *Insurance: Mathematics and Economics*, *118*, 72–94.

Bekaert, G., & Wu, G. (2000). Asymmetric volatility and risk in equity markets. *The Review of Financial Studies*, *13*(1), 1–42.

Biagini, F., Rheinländer, T., & Schreiber, I. (2016). Risk-minimization for life insurance liabilities with basis risk. *Mathematics and Financial Economics*, *10*(2), 151–178.

Biagini, F., Rheinländer, T., & Widenmann, J. (2013). Hedging mortality claims with longevity bonds. *ASTIN Bulletin: The Journal of the IAA*, *43*(2), 123–157.

Blake, D. (2018). Longevity: A new asset class. *Journal of Asset Management*, *19*(5), 278–300.

Blake, D., Cairns, A. J. G., Dowd, K., & Kessler, A. R. (2019). Still living with mortality: The longevity risk transfer market after one decade. *British Actuarial Journal*, *24*(e1), 1–80.

Blake, D., & Burrows, W. (2001). Survivor bonds: Helping to hedge mortality risk. *Journal of Risk and Insurance*, *68*(2), 338–348.

Brown, J. R. (2007). *Rational and behavioral perspectives on the role of annuities in retirement planning*. National Bureau of Economic Research Working Paper 13537.

Cairns, A. J. G. (2011). Modelling and management of longevity risk: Approximations to survivor functions and dynamic hedging. *Insurance: Mathematics and Economics*, *49*, 438–453.

Cairns, A. J. G. (2013). Robust hedging of longevity risk. *Journal of Risk and Insurance*, *80*, 621–648.

Cairns, A. J. G., Blake, D., & Dowd, K. (2006). A two-factor model for stochastic mortality with parameter uncertainty: Theory and calibration. *Journal of Risk and Insurance*, *73*(4), 687–718.

Cairns, A. J. G., Blake, D., & Dowd, K. (2008). Modelling and management of mortality risk: A review. *Scandinavian Actuarial Journal*, *2008*(2–3), 79–113.

Cairns, A. J. G., Blake, D., Dowd, K., Coughlan, G. D., & Khalaf-Allah, M. (2011). Bayesian stochastic mortality modelling for two populations. *ASTIN Bulletin: The Journal of the IAA*, *41*, 29–59.

Cairns, A. J. G., Dowd, K., Blake, D., & Coughlan, G. D. (2014). Longevity hedge effectiveness: A decomposition. *Quantitative Finance*, *14*(2), 217–235.

Chen, A., Guillen, M., & Rach, M. (2021). Fees in tontines. *Insurance: Mathematics and Economics*, *100*, 89–106.

Chen, A., Hieber, P., & Rach, M. (2021). Optimal retirement products under subjective mortality beliefs. *Insurance: Mathematics and Economics*, *101A*, 55–69.

Coughlan, G., Blake, D., MacMinn, R., Cairns, A. J. G., & Dowd, K. (2013). Longevity risk and hedging solutions. *Handbook of Insurance*. New York: Springer. https://doi.org/10.1007/978-1-4614-0155-1_34

Coughlan, G., Epstein, D., Sinha, A., & Honig, P. (2007). *q*-forwards: Derivatives for transferring longevity and mortality. Available at: https://www.researchgate.net/profile/Guy-Coughlan/publication/256109844_q-Forwards_Derivatives_for_Transferring_Longevity_and_Mortality_Risks/links/00463521c8e5387008000000/q-Forwards-Derivatives-for-Transferring-Longevity-and-Mortality-Risks.pdf

Coughlan, G. D., Khalaf-Allah, M., Ye, Y., Kumar, S., Cairns, A. J. G., Blake, D., & Dowd, K. (2011). Longevity hedging 101: A framework for longevity basis risk analysis and hedge effectiveness. *North American Actuarial Journal*, *15*(2), 150–176.

Dahl, M., Melchior, M., & Møller, T. (2008). On systematic mortality risk and risk-minimization with survivor swaps. *Scandinavian Actuarial Journal*, *2008*(2–3), 114–146.

Dahl, M., & Møller, T. (2006). Valuation and hedging of life insurance liabilities with systematic mortality risk. *Insurance: Mathematics and Economics*, *39*(2), 193–217.

Denuit, M. M. (2009). An index for longevity risk transfer. *Journal of Computational and Applied Mathematics*, *230*(2), 411–417.

Doan, B., Papageorgiou, N., Reeves, J. J., & Sherris, M. (2018). Portfolio management with targeted constant market volatility. *Insurance: Mathematics and Economics*, *83*(2018), 134–147.

Donnelly, C., Guillén, M., & Nielsen, J. P. (2014). Bringing cost transparency to the life annuity market. *Insurance: Mathematics and Economics*, *56*, 14–27.

Dowd, K. (2003). Survivor bonds: A comment on Blake and Burrows. *Journal of Risk and Insurance*, *70*(2), 339–348.

Dowd, K., Blake, D., Cairns, A. J. G., & Dawson, P. (2006). Survivor swaps. *Journal of Risk and Insurance*, *73*(1), 1–17.

Evans, J., & Sherris, M. (2010). Longevity risk management and the development of a life Annuity Market in Australia. *Australian School of Business Research Paper No. 2010ACTL0*, 1.

Feller, W. (1951). Two singular diffusion problems. *Annals of Mathematics*, *54*(1), 173–182.

Feng, R., Jing, X., & Ng, K. T. H. (2025). Optimal investment-withdrawal strategy for variable annuities under a performance fee structure. *Journal of Economic Dynamics and Control*, *170*, 105003.

Fishburn, P. C. (1977). Mean-risk analysis with risk associated with below-target returns. *The American Economic Review*, *67*(2), 116–126.

Fortuin, C. M., Kasteleyn, P. W., & Ginibre, J. (1971). Correlation inequalities on some partially ordered sets. *Communications in Mathematical Physics*, *22*(2), 89–103.

Friedman, B. M., & Warshawsky, M. J. (1990). The cost of annuities: Implications for saving behavior and bequests. *The Quarterly Journal of Economics*, *105*(1), 135–154.

Hanewald, K., Piggott, J., & Sherris, M. (2013). Individual post-retirement longevity risk management under systematic mortality risk. *Insurance: Mathematics and Economics*, *52*(1), 87–97.

Heston, S. L. (1993). A closed-form solution for options with stochastic volatility with applications to bond and currency options. *The Review of Financial Studies*, *62*(2), 327–343.

Hull, J. C., & Basu, S. (2016). *Options, futures, and other derivatives*. Pearson Education India.

Human Mortality Database (2024). Max Planck Institute for Demographic Research (Germany), University of California, Berkeley (USA), and French Institute for Demographic Studies (France). Available at: https://www.mortality.org/

Howard, C. T., & D'Antonio, L. J. (1984). A risk-return measure of hedging effectiveness. *Journal of Financial and Quantitative Analysis*, *19*, 101–112.

Hurd, M. D. (1989). Mortality risk and bequests. *Econometrica*, *57*(4), 779–813.

Hyndman, R. (2023). Demography: Forecasting Mortality, Fertility, Migration, and Population Data. Available at: https://pkg.robjhyndman.com/demography/

Kabuche, D., Sherris, M., Villegas, A. M., & Ziveyi, J. (2024). Pooling functional disability and mortality in long-term care insurance and care annuities: A matrix approach for multi-state pools. *Insurance: Mathematics and Economics*, *116*, 165–188.

Kleinow, T. (2015). A common age effect model for the mortality of multiple populations. *Insurance: Mathematics and Economics*, *63*, 147–152.

Konicz, A. K., & Mulvey, J. M. (2015). Optimal savings management for individuals with defined contribution pension plans. *European Journal of Operational Research*, *243*(1), 233–247.

Kroner, K. F., & Sultan, J. (1993). Time-varying distributions and dynamic hedging with foreign currency futures. *Journal of Financial and Quantitative Analysis*, *28*(4), 535–551.

Lee, R. D., & Carter, L. R. (1992). Modeling and forecasting US mortality. *Journal of the American Statistical Association*, *87*(419), 659–671.

Li, J. S., & Hardy, M. (2011). Measuring basis risk in longevity hedges. *North American Actuarial Journal*, *15*(2), 177–200.

Li, S., Labit Hardy, H., Sherris, M., & Villegas, A. M. (2022). A managed volatility investment strategy for pooled annuity products. *Risks*, *10*(6), 121.

Li, N., & Lee, R. (2005). Coherent mortality forecasts for a group of populations: An extension of the Lee-Carter method. *Demography*, *42*, 575–594.

Li, J. S., & Luo, A. (2012). Key q-duration: A framework for hedging longevity risk. *ASTIN Bulletin: The Journal of the IAA*, *42*, 413–452.

Li, J. S., Zhou, R., & Hardy, M. (2015). A step-by-step guide to building two-population stochastic mortality models. *Insurance: Mathematics and Economics*, *63*, 121–134.

Li, J. S., Zhou, R., Liu, Y., Graziani, G., Hall, R. D., Haid, J., Peterson, A., & Pinzur, L. (2020). Drivers of mortality dynamics: Identifying age/period/cohort components of historical US mortality improvements. *North American Actuarial Journal*, *24*(2), 228–250.

Lin, Y., Tan, K. S., Tian, R., & Yu, J. (2014). Downside risk management of a defined benefit plan considering longevity basis risk. *North American Actuarial Journal*, *18*(1), 68–86.

Luciano, E., Regis, L., & Vigna, E. (2012). Delta-gamma hedging of mortality and interest rate risk. *Insurance: Mathematics and Economics*, *50*(3), 402–412.

Mantilla-Garcia, D., Martellini, L., Garcia-Huitrón, M. E., & Martinez-Carrasco, M. A. (2024). Back to the funding ratio! *Addressing the duration puzzle and retirement income risk of defined contribution pension plans. Journal of Banking and Finance*, *159*, 107061.

Markowitz, H. (1952). Portfolio selection. *The Journal of Finance*, *7*(1), 77–91.

Milevsky, M. A. (2014). Portfolio choice and longevity risk in the last seventeenth century. *A re-examination of the first English tontine. Financial History Review*, *21*(3), 225–258.

Milevsky, M. A., & Salisbury, T. S. (2015). Optimal retirement income tontines. *Insurance: Mathematics and Economics*, *64*, 91–105.

Ngai, A., & Sherris, M. (2011). Longevity risk management for life and variable annuities: The effectiveness of static hedging using longevity bonds and derivatives. *Insurance: Mathematics and Economics*, *49*(1), 100–114.

Oehlert, G. W. (1992). A note on the Delta method. *The American Statistician*, *46*(1), 27–29.

Olivieri, A., Thirurajah, S., & Ziveyi, J. (2022). Target volatility strategies for group self-annuity portfolios. *ASTIN Bulletin: The Journal of the IAA*, *52*(2), 591–617.

Owadally, I., Jang, C., & Clare, A. (2021). Optimal investment for a retirement plan with deferred annuities allowing for inflation and labour income risk. *European Journal of Operational Research*, *295*(3), 1132–1146.

Piggott, J., Valdez, E. A., & Detzel, B. (2005). The simple analytics of a pooled annuity fund. *Journal of Risk and Insurance*, *72*(3), 497–520.

Pitacco, E. (2016). Guarantee structures in life annuities: A comparative analysis. *The Geneva Papers on Risk and Insurance - Issues and Practice*, *41*(1), 78–97.

Qiao, C., & Sherris, M. (2013). Managing systematic mortality risk with group self-pooling and annuitization schemes. *Journal of Risk and Insurance*, *80*(4), 949–974.

Rosa, C. D., Luciano, E., & Regis, L. (2017). Basis risk in static versus dynamic longevity-risk hedging. *Scandinavian Actuarial Journal*, *2017*(4), 343–365.

Roy, A. D. (1952). Safety first and the holding of assets. *Econometrica*, *20*(3), 431–449.

Sharpe, W. F. (1994). The sharpe ratio. *Journal of Portfolio Management*, *21*(1), 49–58.
Shen, Y., Sherris, M., Wang, Y., & Ziveyi, J. (2023). The valuation and assessment of retirement income products: A unified Markov chain Monte Carlo framework. UNSW Business School Research Paper Forthcoming, Available at SSRN: https://ssrn.com/abstract=4595961
Sherris, M., Xu, Y., & Ziveyi, J. (2020). Cohort and value-based multi-country longevity risk management. *Scandinavian Actuarial Journal*, *2020*(7), 650–676.
Stamos, M. Z. (2008). Optimal consumption and portfolio choice for pooled annuity funds. *Insurance: Mathematics and Economics*, *43*(1), 56–68.
Tan, C. I., Li, J., Li, J. S., & Balasooriya, U. (2014). Parametric mortality indexes: From index construction to hedging strategies. *Insurance Mathematics and Economics*, *59*(C), 285–299.
Tan, K. S., Weng, C., & Zhang, J. (2022). Optimal dynamic longevity hedge with basis risk. *European Journal of Operational Research*, *297*, 325–337.
Tang, S., & Li, J. (2021). Market pricing of longevity-linked securities. *Scandinavian Actuarial Journal*, *5*, 408–436.
Valdez, E. A., Piggott, J., & Wang, L. (2006). Demand and adverse selection in a pooled annuity fund. *Insurance: Mathematics and Economics*, *39*(2), 251–266.
Weinert, J., & Gründl, H. (2021). The modern tontine. *European Actuarial Journal*, *11*, 49–86.
World Health Organization 2024. World health statistics 2024: Monitoring health for the SDGs, sustainable development goals. Available at: https://www.who.int/publications/i/item/9789240094703
Wong, T. W., Chiu, M. C., & Wong, H. Y. (2014). Time-consistent mean-variance hedging of longevity risk: Effect of cointegration. *Insurance: Mathematics and Economics*, *56*, 56–67.
Wong, T. W., Chiu, M. C., & Wong, H. Y. (2017). Managing mortality risk with longevity bonds when mortality rates are cointegrated. *Journal of Risk and Insurance*, *84*(3), 987–1023.
Wu, G. (2001). The determinants of asymmetric volatility. *The Review of Financial Studies*, *14*(3), 837–859.
Yaari, M. E. (1965). Uncertain lifetime, life insurance, and the theory of the consumer. *Review of Economic Studies*, *32*(2), 137–150.
Zhou, K. Q., & Li, J. S. (2017). Dynamic longevity hedging in the presence of population basis risk: A feasibility analysis from technical and economic perspectives. *Journal of Risk and Insurance*, *2017*(84), 417–437.
Zhou, K. Q., & Li, J. S. (2019). Delta-hedging longevity risk under the m7-m5 model: The impact of cohort effect uncertainty and population basis risk. *Insurance: Mathematics and Economics*, *84*, 1–21.

How to cite this article: Shen, Y., Sherris, M., Wang, Y., & Ziveyi, J. (2025). Optimal hedging of longevity risks for group self-annuity portfolios. *Journal of Risk and Insurance*, 1–46. https://doi.org/10.1111/jori.70024

APPENDIX A: PROOFS

Proof of proposition 2.1

Proof. Using the tower property of conditional expectation, we have:

$$\begin{aligned}\mathbb{E}_t[P_s(t)] &= (1+r^f)^{-(T^*+t-s)}\mathbb{E}_t\left[\mathbb{E}_s\left[S^{(R)}_{x^f,t}(T^*)\right]-p^f_t\right]\\ &= (1+r^f)^{-(T^*+t-s)}\left\{\mathbb{E}_t\left[S^{(R)}_{x^f,t}(T^*)\right]-p^f_t\right\}\\ &= (1+r^f)^{-(T^*+t-s)}\left\{\mathbb{E}_t\left[S^{(R)}_{x^f,t}(T^*)\right]-(1+\lambda)\mathbb{E}_t\left[S^{(R)}_{x^f,t}(T^*)\right]\right\}\\ &\le 0.\end{aligned}$$

□

Proof of proposition 3.5

Proof. Over the year $[t, t+1)$, the hedging profit or loss, $P_{t+1}(t)$, and the 1-year survival probability of the members, $S^{(F)}_{x+t,t}(1)$, are correlated through the common time-varying index K_{t+1} in the ACF model. Under the assumption that $G_x > 0$ in the ACF model, when there is a decrease in K_{t+1}, the mortality rate $m^{(i)}_{x,t+1}$ decreases, since the following relationship holds:

$$\frac{\partial m^{(i)}_{x,t+1}}{\partial K_{t+1}} = m^{(i)}_{x,t+1} G_x > 0.$$

This will cause an increase in $P_{t+1}(t)$ and $S^{(F)}_{x+t,t}(1)$, which implies $P_{t+1}(t)$ is a decreasing function of K_{t+1} and $\frac{1}{S^{(F)}_{x+t,t}(1)}$ is an increasing function of K_{t+1}.

By applying the Fortuin–Kasteleyn–Ginibre inequality (Fortuin et al., 1971), we have

$$\mathbb{E}_t\left[\frac{P_{t+1}(t)}{S^{(F)}_{x+t,t}(1)}\right] \le \mathbb{E}_t[P_{t+1}(t)]\,\mathbb{E}_t\left[\frac{1}{S^{(F)}_{x+t,t}(1)}\right] \le 0,$$

where we use the result in Proposition 2.1 in the second inequality.

Then, if $h_t > 0$, we have

$$\mathbb{E}_t\left[B^{(H)}_{t+1}\right] = \mathbb{E}_t[B_{t+1}] + \frac{h_t}{N_t}\mathbb{E}_t\left[\frac{P_{t+1}(t)}{S^{(F)}_{x+t,t}(1)}\right] \le \mathbb{E}_t[B_{t+1}].$$

Similarly, the result for the other direction holds. □

Proof of proposition 3.8

Proof. From the proof of Proposition 3.5, we know:

$$\mathbb{E}_t\left[B^{(H)}_{t+1}\right] = \mathbb{E}_t[B_{t+1}] + \frac{h_t}{N_t}\mathbb{E}_t\left[\frac{P_{t+1}(t)}{S^{(F)}_{x+t,t}(1)}\right].$$

Then

$$\frac{h_t}{N_t} = \frac{\mathbb{E}_t\left[B^{(H)}_{t+1}\right] - \mathbb{E}_t[B_{t+1}]}{\mathbb{E}_t\left[\frac{P_{t+1}(t)}{S^{(F)}_{x+t,t}(1)}\right]}. \tag{A1}$$

Consequently, by Equations (10) and (A1), we can rewrite $\mathrm{Var}_t\left[B^{(H)}_{t+1}\right]$ into:

$$\begin{aligned}
\mathrm{Var}_t\left[B_{t+1}^{(H)}\right] &= \mathrm{Var}_t\left[B_{t+1} + \frac{h_t P_{t+1}(t)}{N_t S_{x+t,t}^{(F)}(1)}\right] \\
&= \mathrm{Var}_t[B_{t+1}] + 2\frac{h_t}{N_t}\mathrm{Cov}_t\left[B_{t+1}, \frac{P_{t+1}(t)}{S_{x+t,t}^{(F)}(1)}\right] + \frac{h_t^2}{N_t^2}\mathrm{Var}_t\left[\frac{P_{t+1}(t)}{S_{x+t,t}^{(F)}(1)}\right] \\
&= \mathrm{Var}_t[B_{t+1}] + 2\frac{\mathbb{E}_t\left[B_{t+1}^{(H)}\right] - \mathbb{E}_t[B_{t+1}]}{\mathbb{E}_t\left[\frac{P_{t+1}(t)}{S_{x+t,t}^{(F)}(1)}\right]}\mathrm{Cov}_t\left[B_{t+1}, \frac{P_{t+1}(t)}{S_{x+t,t}^{(F)}(1)}\right] \\
&\quad + \left(\frac{\mathbb{E}_t\left[B_{t+1}^{(H)}\right] - \mathbb{E}_t[B_{t+1}]}{\mathbb{E}_t\left[\frac{P_{t+1}(t)}{S_{x+t,t}^{(F)}(1)}\right]}\right)^2 \mathrm{Var}_t\left[\frac{P_{t+1}(t)}{S_{x+t,t}^{(F)}(1)}\right] \\
&= A_{1,t}\left(\mathbb{E}_t\left[B_{t+1}^{(H)}\right]\right)^2 + A_{2,t}\mathbb{E}_t\left[B_{t+1}^{(H)}\right] + A_{3,t}.
\end{aligned} \tag{A2}$$

Note that Equation (A2) is a quadratic function of h_t, applying the first-order condition with respect to h_t yields:

$$h_t^{(GMVP)} = -\mathrm{Corr}_t\left[\frac{P_{t+1}(t)}{N_{t+1}}, B_{t+1}\right]\frac{\mathrm{Std}_t[B_{t+1}]}{\mathrm{Std}_t\left[\frac{P_{t+1}(t)}{N_{t+1}}\right]}.$$

□

Proof of proposition 3.12

Proof. Since

$$V_t(h_t) := \mathrm{Var}_t\left[B_{t+1}^{(H)}\right] - 2\phi_t\left(\mathbb{E}_t\left[B_{t+1}^{(H)}\right] - \mathbb{E}_t[B_{t+1}]\right)$$

is the value function, the GSA members try to minimize. We use Equation (10) to write the value function as:

$$\begin{aligned}
V_t(h_t) &= \mathrm{Var}_t\left[B_{t+1} + \frac{h_t P_{t+1}(t)}{N_{t+1}}\right] - 2\phi_t\mathbb{E}_t\left[B_{t+1} + \frac{h_t P_{t+1}(t)}{N_{t+1}}\right] + 2\phi_t\mathbb{E}_t[B_{t+1}] \\
&= 2h_t\mathrm{Cov}_t\left[B_{t+1}, \frac{P_{t+1}(t)}{N_{t+1}}\right] + h_t^2\mathrm{Var}_t\left[\frac{P_{t+1}(t)}{N_{t+1}}\right] - 2h_t\phi_t\mathbb{E}_t\left[\frac{P_{t+1}(t)}{N_{t+1}}\right] \\
&\quad + \mathrm{Var}_t[B_{t+1}].
\end{aligned}$$

The value function is a quadratic function of h_t and applying the first-order condition with respect to h_t yields:

$$\frac{\partial V_t(h_t)}{\partial h_t} = 2\mathrm{Cov}_t\left[B_{t+1}, \frac{P_{t+1}(t)}{N_{t+1}}\right] + 2h_t \mathrm{Var}_t\left[\frac{P_{t+1}(t)}{N_{t+1}}\right] - 2\phi_t \mathbb{E}_t\left[\frac{P_{t+1}(t)}{N_{t+1}}\right] = 0.$$

Then we obtain

$$h_t^*\left(F_t^+, N_t, K_t, k_t^{(F)}, k_t^{(R)}, \phi_t\right) = \frac{\phi_t \mathbb{E}_t\left[\frac{P_{t+1}(t)}{N_{t+1}}\right] - \mathrm{Cov}_t\left[\frac{P_{t+1}(t)}{N_{t+1}}, B_{t+1}\right]}{\mathrm{Var}_t\left[\frac{P_{t+1}(t)}{N_{t+1}}\right]}.$$

Solving $h_t^*(\phi_t^{(RN)}) = 0$ yields:

$$\phi_t^{(RN)}\left(F_t^+, N_t, K_t, k_t^{(F)}, k_t^{(R)}\right) = \frac{\mathrm{Cov}_t\left[\frac{P_{t+1}(t)}{N_{t+1}}, B_{t+1}\right]}{\mathbb{E}_t\left[\frac{P_{t+1}(t)}{N_{t+1}}\right]} = A_{4,t}.$$

□

Proof of proposition 5.2

Proof. Let Y_t^f and T^f be the price and maturity of the future on equity. No arbitrage condition yields:

$$Y_t^f = (1 + r^f)^{T^f - t} Y_t.$$

Applying Itô's lemma, we obtain:

$$dY_t^f = (1 + r^f)^{T^f - t} dY_t - (1 + r^f)^{T^f - t} Y_t \log(1 + r^f) dt.$$

Then

$$\begin{aligned}\frac{dY_t^f}{Y_t^f} &= \frac{(1 + r^f)^{T^f - t} dY_t - (1 + r^f)^{T^f - t} Y_t \log(1 + r^f) dt}{(1 + r^f)^{T^f - t} Y_t}, \\ &= \frac{dY_t}{Y_t} - \log(1 + r^f) dt.\end{aligned}$$

The instantaneous return of the Type B strategy is:

$$\begin{aligned}r_t &= \frac{dY_t}{Y_t} + (w_t - 1)\frac{dY_t^f}{Y_t^f}, \\ &= \frac{dY_t}{Y_t} + (w_t - 1)\left(\frac{dY_t}{Y_t} - \log(1 + r^f) dt\right), \\ &= w_t \frac{dY_t}{Y_t} + (1 - w_t)\log(1 + r^f) dt,\end{aligned}$$

where the last line is the instantaneous return of the Type A strategy. This completes the proof. □

APPENDIX B: APPROXIMATION FOR SPOT SURVIVAL PROBABILITY

By Cairns (2011) and Zhou and Li (2017), the spot survival probability $p_{x,t}^{(i)}\left(s, K_t, k_t^{(i)}\right)$ in Equation (4) can be determined as:

$$p_{x,t}^{(i)}\left(s, K_t, k_t^{(i)}\right) = \Phi\left(f_{x,t}^{(i)}\left(s, K_t, k_t^{(i)}\right)\right),$$

where $\Phi(\cdot)$ is the standard normal distribution function and

$$f_{x,t}^{(i)}\left(s, K_t, k_t^{(i)}\right) := \Phi^{-1}\left(p_{x,t}^{(i)}\left(s, K_t, k_t^{(i)}\right)\right)$$

is the probit transform of the spot survival probability.

Let $\hat{K}_t := \mathbb{E}[K_t|K_0]$ and $\hat{k}_t^{(i)} := \mathbb{E}[\hat{k}_t^{(i)}|\hat{k}_0^{(i)}]$. Then $f_{x,t}^{(i)}(s, K_t, k_t^{(i)})$ can be approximated by its second-order Taylor series expansion $\tilde{f}_{x,t}^{(i)}(s, K_t, k_t^{(i)})$ around $(\hat{K}_t, \hat{k}_t^{(i)})$ as:

$$\begin{aligned}\tilde{f}_{x,t}^{(i)}\left(s, K_t, k_t^{(i)}\right) := {} & \gamma_{x,t,0}^{(i)}(s) + \gamma_{x,t,1}^{(i)}(s)(K_t - \hat{K}_t) + \gamma_{x,t,2}^{(i)}(s)\left(k_t^{(i)} - \hat{k}_t^{(i)}\right) \\ & + \frac{1}{2}\gamma_{x,t,3}^{(i)}(s)(K_t - \hat{K}_t)^2 + \frac{1}{2}\gamma_{x,t,4}^{(i)}(s)\left(k_t^{(i)} - \hat{k}_t^{(i)}\right)^2 \\ & + \gamma_{x,t,5}^{(i)}(s)(K_t - \hat{K}_t)\left(k_t^{(i)} - \hat{k}_t^{(i)}\right),\end{aligned}$$

where

$$\gamma_{x,t,0}^{(i)}(s) = f_{x,t}^{(i)}\left(s, K_t, k_t^{(i)}\right), \quad \gamma_{x,t,1}^{(i)}(s) = \left.\frac{\partial f_{x,t}^{(i)}\left(s, K_t, k_t^{(i)}\right)}{\partial K_t}\right|_{K_t=\hat{K}_t},$$

$$\gamma_{x,t,2}^{(i)}(s) = \left.\frac{\partial f_{x,t}^{(i)}\left(s, K_t, k_t^{(i)}\right)}{\partial k_t^{(i)}}\right|_{k_t^{(i)}=\hat{k}_t^{(i)}}, \quad \gamma_{x,t,3}^{(i)}(s) = \left.\frac{\partial^2 f_{x,t}^{(i)}\left(s, K_t, k_t^{(i)}\right)}{\partial K_t^2}\right|_{K_t=\hat{K}_t},$$

$$\gamma_{x,t,4}^{(i)}(s) = \left.\frac{\partial^2 f_{x,t}^{(i)}\left(s, K_t, k_t^{(i)}\right)}{\partial \left(k_t^{(i)}\right)^2}\right|_{k_t^{(i)}=\hat{k}_t^{(i)}}, \quad \gamma_{x,t,5}^{(i)}(s) = \left.\frac{\partial^2 f_{x,t}^{(i)}\left(s, K_t, k_t^{(i)}\right)}{\partial K_t \partial k_t^{(i)}}\right|_{K_t=\hat{K}_t, k_t^{(i)}=\hat{k}_t^{(i)}}.$$

A key feature of the approximation method is that the partial derivatives $\gamma_{x,t,j}^{(i)}(s)$ for $j = 0, 1, ..., 5$ are independent of the realized mortality path. We first compute the partial derivatives through finite difference approximation (Cairns, 2011), then use the partial derivatives to approximate the spot survival probabilities to avoid nested Monte Carlo.

APPENDIX C: HEDGE EFFECTIVENESS WHEN *S*-FORWARDS ARE FAIRLY PRICED

This appendix presents the hedging results when the S-forwards are fairly priced, that is, when no risk premium is charged and $\lambda = 0$. Comparing Table C1 with the results in Table 2, the risk

premium mainly increases MRR, while its effect on VRR is minimal. This is because the risk premium reduces the hedging profit or loss $P_{t+1}(t)$ linearly, and the correlation between $\frac{P_{t+1}(t)}{N_{t+1}}$ and B_{t+1} remains unchanged. We also observe a decrease in the optimal value function in Table C2, suggesting fund members benefit from the longevity hedge.

TABLE C1 The variance and mean reduction ratios of the hedge at selected ages ($\alpha = 0.8, \beta = 0$, and $\lambda = 0$).

Age	Mean	Minimum	Maximum	95% confidence interval
Variance reduction ratio				
65	95.90%	95.89%	95.90%	(95.89%, 95.90%)
70	95.92%	95.89%	95.94%	(95.91%, 95.93%)
75	95.95%	95.93%	95.96%	(95.94%, 95.95%)
80	95.92%	95.91%	95.93%	(95.92%, 95.93%)
85	94.75%	94.23%	95.01%	(94.57%, 94.89%)
90	84.34%	82.76%	85.48%	(83.73%, 84.92%)
95	49.68%	45.78%	53.05%	(47.99%, 51.33%)
Mean reduction ratio				
65	0.00031%	0.00029%	0.00033%	(0.00030%, 0.00032%)
70	0.00047%	0.00027%	0.00079%	(0.00036%, 0.00061%)
75	0.00071%	0.00032%	0.00145%	(0.00049%, 0.00098%)
80	0.00103%	0.00043%	0.00225%	(0.00068%, 0.00149%)
85	0.00142%	0.00068%	0.00285%	(0.00097%, 0.00198%)
90	0.00163%	0.00076%	0.00333%	(0.00114%, 0.00221%)
95	0.00134%	0.00080%	0.00205%	(0.00107%, 0.00166%)

TABLE C2 The impact of longevity hedge on the optimal value function at selected ages ($\alpha = 0.8, \beta = 0$, and $\lambda = 0$).

Age	Mean	Minimum	Maximum	95% confidence interval
Optimal longevity hedge				
65	9.01	8.51	9.58	(8.76, 9.26)
70	9.15	5.11	15.34	(7.03, 11.75)
75	9.26	4.50	20.20	(6.31, 13.19)
80	9.67	3.72	27.90	(5.81, 15.18)
85	10.07	3.87	34.08	(5.99, 16.23)
90	12.71	3.76	50.92	(6.80, 21.85)
95	27.31	9.25	79.31	(16.09, 44.30)

(Continues)

TABLE C2 (Continued)

Age	Mean	Minimum	Maximum	95% confidence interval
Without longevity hedge				
65	24.97	23.58	26.57	(24.28, 25.66)
70	25.39	14.18	42.53	(19.52, 32.59)
75	25.70	12.49	56.03	(17.51, 36.59)
80	26.83	10.31	77.38	(16.13, 42.12)
85	27.32	10.56	91.65	(16.31, 43.91)
90	29.03	8.39	114.66	(15.48, 49.85)
95	40.80	13.78	115.90	(24.09, 65.78)

APPENDIX D: RISK DECOMPOSITION

This appendix presents a risk decomposition method. Let r_{t+1} be the investment return during the period $[t, t+1)$, the survival benefit at time $t+1$ is expressed as:

$$B_{t+1}(\Theta_{t+1}) = \frac{F_t^+(1+r_{t+1})}{\ddot{a}^e_{x+t+1,t+1}N_{t+1}}, \tag{D1}$$

where $\Theta_{t+1} := \left(K_{t+1}, k_{t+1}^{(F)}, r_{t+1}\right)^\top$ is the set of risks including the systematic longevity risk $\left\{K_{t+1}, k_{t+1}^{(F)}\right\}$ and the investment risk r_{t+1}, and $^\top$ is a transpose operator on a vector or matrix.

Using the delta method (Oehlert, 1992), we can approximate the variance of $B_{t+1}(\Theta_{t+1})$ as:

$$\mathrm{Var}_t[B_{t+1}(\Theta_{t+1})] \approx \nabla B_{t+1}(\Theta)^\top|_{\Theta=\mathbb{E}_t(\Theta_{t+1})} \times \Sigma_t \times \nabla B_{t+1}(\Theta)|_{\Theta=\mathbb{E}_t(\Theta_{t+1})},$$

where

$$\nabla B_{t+1}(\Theta) = \begin{pmatrix} \dfrac{\partial B_{t+1}(\Theta_{t+1})}{\partial K_{t+1}} \\ \dfrac{\partial B_{t+1}(\Theta_{t+1})}{\partial k_{t+1}^{(F)}} \\ \dfrac{\partial B_{t+1}(\Theta_{t+1})}{\partial r_{t+1}} \end{pmatrix}, \Sigma_t = \begin{pmatrix} \mathrm{Var}_t(K_{t+1}) & \mathrm{Cov}_t\left(K_{t+1}, k_{t+1}^{(F)}\right) & \mathrm{Cov}_t(K_{t+1}, r_{t+1}) \\ \mathrm{Cov}_t\left(K_{t+1}, k_{t+1}^{(F)}\right) & \mathrm{Var}_t\left(k_{t+1}^{(F)}\right) & \mathrm{Cov}_t\left(k_{t+1}^{(F)}, r_{t+1}\right) \\ \mathrm{Cov}_t(K_{t+1}, r_{t+1}) & \mathrm{Cov}_t\left(k_{t+1}^{(F)}, r_{t+1}\right) & \mathrm{Var}_t(r_{t+1}) \end{pmatrix}.$$

Since the financial markets and the mortality dynamics are assumed to be independent, the covariance matrix Σ_t can be simplified as:

$$\Sigma_t = \begin{pmatrix} \mathrm{Var}_t(K_{t+1}) & 0 & 0 \\ 0 & \mathrm{Var}_t\left(k_{t+1}^{(F)}\right) & 0 \\ 0 & 0 & \mathrm{Var}_t(r_{t+1}) \end{pmatrix}.$$

By Equation (D1), the derivative $\frac{\partial B_{t+1}(\Theta_{t+1})}{\partial r_{t+1}}$ can be calculated directly as:

$$\frac{\partial B_{t+1}(\Theta_{t+1})}{\partial r_{t+1}} = \frac{F_t^+}{\ddot{a}^e_{x+t+1,t+1} N_{t+1}}.$$

Then INV_t can be determined as:

$$\mathrm{INV}_t := \left(\frac{\partial B_{t+1}(\Theta_{t+1})}{\partial r_{t+1}} \bigg|_{\Theta = \mathbb{E}_t(\Theta_{t+1})} \right)^2 \mathrm{Var}_t(r_{t+1}),$$

and the systematic longevity risk component can be determined as:

$$\mathrm{LONG}_t = \mathrm{Var}_t[B_{t+1}(\Theta_{t+1})] - \mathrm{INV}_t,$$

where we numerically evaluate the total variance $\mathrm{Var}_t[B_{t+1}(\Theta_{t+1})]$.

APPENDIX E: ESTIMATES OF PARAMETERS IN THE ACF MODEL

Figure E1 depicts the parameter estimates for the ACF model. The time-varying index K_t in the common factor shows a decreasing trend, and mortality rates for the two populations are

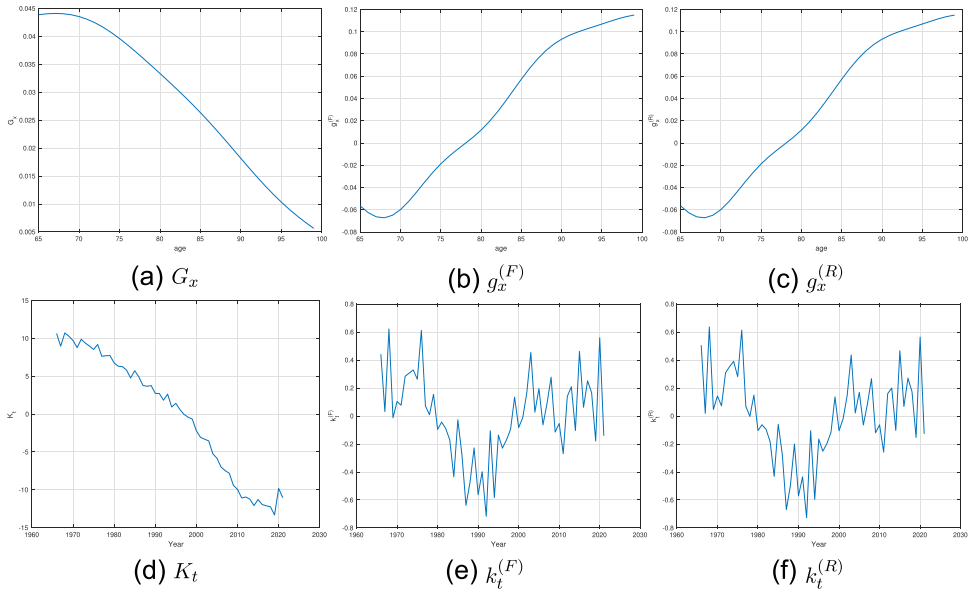

FIGURE E1 The fitted ACF model for the unisex mortality data of the England and Wales total population and the United Kingdom total population aged from 65 to 99 over the period from 1966 to 2021.

improving. The shape parameter G_x in the common factor also shows a downward trend, and the younger population gain more mortality improvement than the older population. Meanwhile, G_x is positive for the population aged from 65 to 99 and our assumption in Proposition 3.5 is satisfied. From the plots of the population-specific time-varying indices $k_t^{(F)}$ and $k_t^{(R)}$, we observe a mean-reverting trend. This property guarantees the mortality projections of the two populations are coherent and do not diverge to infinity (Li & Lee, 2005).